ABSTRACT

Title of Document: BACTERIAL PHENOTYPES AND MOLECULAR MECHANISMS OF MECHANOSENSITIVE CHANNELS

Lena Alma Shirinian, Master of Science, 2005

Directed By: Associate Professor, Sergei Sukharev, Department of Biology

This work presents a functional analysis of mutations in two bacterial mechanosensitive channels, MscL and MscS using bacterial growth phenotyping combined with electrophysiological and structural analyses. The introduction of aromatic caps at the ends of lipid facing helices in MscL compromises the osmotic rescuing function of the channel and changes gating parameters. The characteristic absence of aromatic residues at membrane interfaces is critical for MscL function, as the opening transition is associated with a strong helical reorientation. According to the current model of MscS, the pore-forming TM3 helices are predicted to separate, tilt, and straighten upon channel opening. This dynamic transition has been examined using a cysteine scan of this region and MTS accessibility experiments. Both cell viability assays and electrophysiological data support the hypothesis of a helical separation. Conductance measurements in gate mutants suggest that the pore lumen narrows toward the periplasmic end, consistent with the current model.

# BACTERIAL PHENOTYPES AND MOLECULAR MECHANISMS OF MECHANOSENSITIVE CHANNELS

By

Lena Alma Shirinian

Thesis submitted to the Faculty of the Graduate School of the
University of Maryland, College Park, in partial fulfillment
of the requirements for the degree of
Master of Science
2005

Advisory Committee:
Dr. Sergei Sukhavev, Chair
Dr. Marco Colombini
Dr. Hey-Kyoung Lee

© Copyright by
Lena Alma Shirinian
2005

# Preface

The following work represents a collaborative effort within our laboratory. Drs. Chien-Sung Chiang and Sergei Sukharev provided the majority of the electrophysiological data. Structural figures and molecular simulations were kindly provided by Dr. Andriy Anishkin. The remainder of the figures and the following text is a result of three years of research as a graduate student at the University of Maryland, College Park.

# Acknowledgements

First and foremost I would like to thank Dr. Sergei Sukharev for his guidance and support over the years. He has enabled me to become a confident and knowledgeable researcher who loves to be in the laboratory. I am very grateful for the experience and skills I have obtained in your lab and thank you wholly for the opportunity.

I would also like to thank Dr. Marco Colombini, not only for his support but also for motivating me to think about the reason behind my research. I thank you for being so helpful and available when I needed your guidance and help. I sincerely thank you for your assistance throughout my studies here.

Dr. Hey-Kyoung Lee, thank you for your time and willingness to serve on my committee. Your class provided me with the knowledge of many new techniques which I will use throughout my career.

Andriy and Chien-Sung, thank you for helping me with my research and for providing data and figures to accompany my own. You have been a great help.

Lois, I could write a page and it would not be enough, you have been so helpful and so supportive to me all these years. I cannot thank you enough.

# Table of Contents

Acknowledgements ..... iii
List of Abbreviations ..... v
List of Tables ..... vi
List of Figures ..... vii
Chapter 1: Introduction ..... 1
Mechanosensitive Channels ..... 1
Background ..... 3
MscL ..... 5
MscS ..... 7
Physiological Approaches to MS Channel Mechanisms ..... 9
GOF Phenotypes ..... 9
MTS Accessibility ..... 11
LOF Mutations and Second-site Suppressors of GOF Mutations ..... 13
Rationale for Further Investigation ..... 14
Chapter 2: Materials and Methods ..... 17
Strains and Molecular Modifications ..... 17
MscL ..... 17
MscS ..... 18
Control of Protein Expression ..... 18
MscL ..... 18
MscS ..... 19
Electrophysiology ..... 19
Cell Viability Assays ..... 20
MTS Accessibility Experiments ..... 21
Growth Curves ..... 22
Chapter 3: Capping of MscL Helices ..... 23
Problem Statement ..... 22
Results ..... 28
Protein Expression and Osmotic Survival Assays ..... 28
Channel Gating Parameters ..... 33
Discussion ..... 38
Chapter 4: Dynamics of Pore-Lining Helices in MscS ..... 44
Introduction ..... 44
Results and Discussion ..... 50
Determination of MTS Accessibility of TM3 Residues ..... 50
Characterization of the Overall Geometry of the Open Pore ..... 53
Conclusions ..... 57
References ..... 61

# List of Abbreviations

MS- Mechanosensitive channel

MscS- Mechanosensitive channel of small conductance

MscL- Mechanosensitive channel of large conductance

SCAM- Scanning Cysteine Accessibility Mutagenesis

MTSEA- 2-Aminoethyl methane thiosulfonate Hydrobromide

MTSET- 2-Trimethylammonium ethyl]methanethiosulfonate Bromide

PDVF- Polyvinylidine fluoride

TM- Transmembrane

LOF- Loss of function

GOF- Gain of function

# List of Tables

1. Electrophysiological properties of mutants and osmotic survival……30

# List of Figures

1. Crystal Structures of MscL from *M. tuberculosis* and *E. coli* MscS…….....2

2. Models of the EcoMscL transmembrane barrel in the closed and open states……25

3. Expression levels of mutant proteins and osmotic survival of MJF 455 cells…….32

4. Characteristic fragments of single-channel traces expressing mutant MscLs…….34

5. Single-channel characteristics of selected mutants which deviate from WT...…...36

6. Survival of mutants under low-copy (uninduced) conditions……..37

7. The hypothetical MscS gating transition…….……45

8. Cross-sections of the closed and open conformations……..…46

9. Osmotic survival data of MJF 465 cells with MTS…….51

10. Traces of cysteine mutants in the gate region of TM3…….…..53

11. Arrangement of helices and gate keeping aliphatic residues…….55

12. Traces of gate mutants and I-V curves……..56

# Chapter 1: Introduction

## *Mechanosensitive Channels*

Mechanosensitive channels (MS) are found in all species ranging from viruses and prokaryotes to humans (*1*). In higher organisms they fulfill functions of sensory receptors, while in microorganisms, such as *E. coli*, they provide osmotic protection, acting as osmolyte release valves which activate upon hypotonic shock (*2*). By making specific amino acid substitutions we can elucidate the structure-function relationships and deduce the mechanism of channel function. Several different bacterial phenotypes have been associated with mutations in the bacterial mechanosensitive channels MscL and MscS. For MscL, we would like to understand the specific role of aromatic residues at membrane interfaces by capping the transmembrane helices of MscL with aromatic residues while studying its effect upon gating. And finally, the remainder of the work will focus with MscS in order to give an assessment of the dynamics and spatial positions of pore-lining TM3. By studying both types of channels we will be able to better understand the function these channels play as well as elucidate and verify our hypothetical gating models.

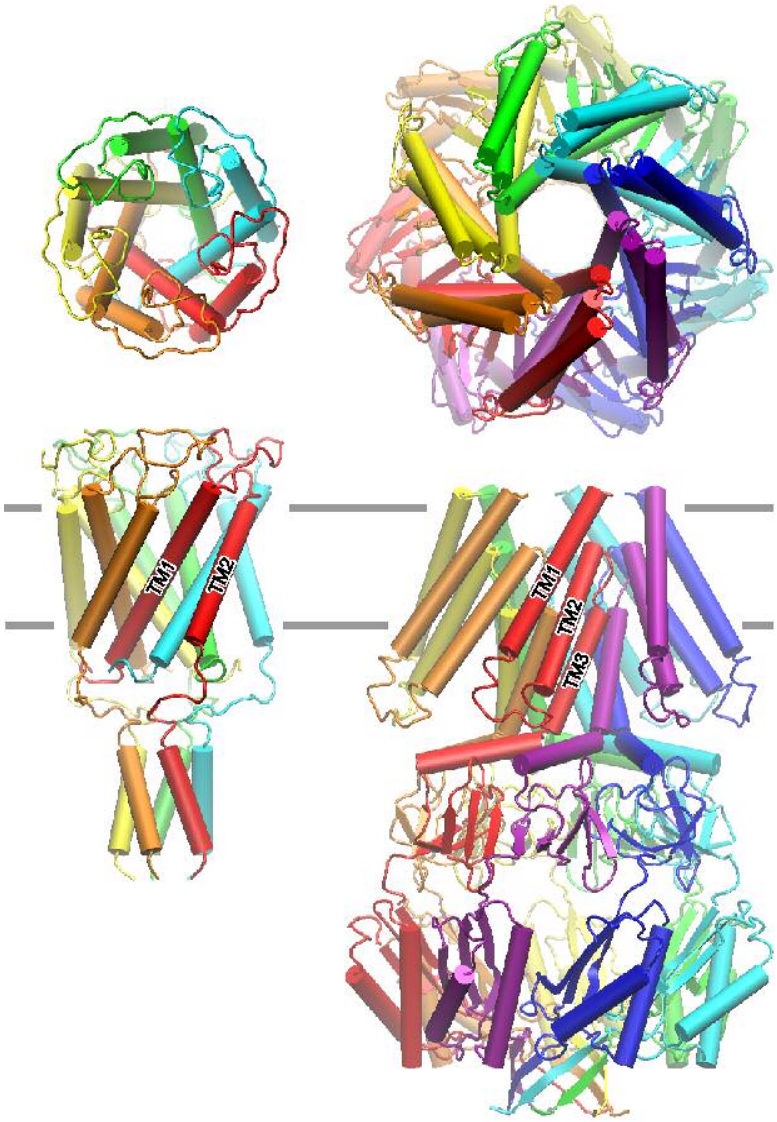


**Figure 1.** Crystal structures of MscL form *M. tuberculosis* (left) and *E. coli* MscS (right). Alpha helical elements are depicted as rods. Each subunit is colored individually to show the topology. Horizontal lines indicate membrane boundaries.

There are three types of MS channels that have been identified in *E. coli,* MscS, MscL, and MscK, which are characterized by both their electrical conductance and the pressure threshold for activation. MscL conducts at a larger conductance of about 3ns (*3*), and MscS, at just 1nS. The two major types of MS channels, MscL and

MscS (Fig. 1), are partially redundant, and function to protect the cell upon osmotic down shock even though they contain no sequence similarity and minimal structural resemblance (*2*). The deletion of both genes results in an osmotically fragile phenotype, resulting in cell lysis upon a 400 mOsM down shock, thus demonstrating that the rapid release of solutes is essential for cell survival upon shock. These studies will involve making amino acid substitutions throughout the gene sequences to allow us to better understand the functional roles that these channels play as well as to identify interaction between functionally important domains within the proteins. The *in vivo* effects of mutations will be characterized by growth rate, plating efficiency, and the rate of survival after osmotic shock. These effects can then be correlated with patterns of single-channel gating observed in patch-clamp experiments. Channel opening at a certain pressure threshold can be directly correlated to survival data. This will allow us to identify functionally important domains and interactions. These channels essentially serve as convenient and structurally-defined models for determining how proteins sense and respond to membrane tension (*4*).

*Background*

Ion channels are membrane proteins found in all living organisms which play important roles in a wide variety of processes such as forming neural connections, signaling, sensation, osmotic balance, and solute transport (*5*). Channels evolved early and are present in unicellular organisms, such as: protists, fungi, bacteria, archaea, and even viruses. Because of their ubiquitous nature and diversity in

processes they mediate, defects in their function may result in marked physiological effects. Mutations in channel genes lead to disorders called *channelopathies*, which may affect protein expression, or may lead to a gain or loss of channel function as a result of a mutation in the coding region of an ion channel gene(*6*). Therefore, if such a channel is a part of a microbial metabolic or stress-response system, its aberrant function is manifested as a growth defect on plates or in liquid cultures under normal conditions or conditions of acute osmotic stress. This approach allows for the detection of such mutations and has been extensively applied in studies of bacterial mechanosensitive channels, allowing us to understand not only the physiology of these channels, but may also directly indicate changes in gating parameters. When used in combination with other methods, such as patch clamp and molecular modeling/simulations, bacterial phenotyping becomes a very powerful approach pointing to functionally important parts and domain interactions.

Mechanosensitive ion channels (MS), more specifically, take part in a number of different processes ranging from volume regulation in bacteria and other cell walled organisms, gravitropism in plants, proprioception, touch sensation, hearing, and cardiovascular regulation in all animals (*7*). In prokaryotes, MS channels fulfill functions of osmotic valves. Their ability to respond to increases in cell volume is critical for all living organisms. This survival mechanism has been best characterized in *Escherichia coli* (*2*). MS channels reside in the cytoplasmic membrane and play a protective role in the regulation of cell volume and turgor pressure upon osmotic stress. Changes in external osmolarity can either cause a cell to shrink or swell depending on whether the concentration of dissolved substances in the medium is

greater or lesser than in the cytoplasm, respectively. An increase in turgor pressure is the result of the accumulation of solutes inside the cell and a decrease in the osmolarity of the surrounding medium (*8*). Cell volume regulation occurs by a simple sequence of events. Osmotic downshift results in a net influx of water and cell swelling. This influx causes an increase in turgor pressure, which without the activation of MS channels would cause the cell to burst. As both turgor pressure and membrane tension build up, the channels open causing osmolytes and water to leave the cell. Upon sufficient down shock, MS channels are activated by an increase in tension in the membrane to combat the effects of changes in osmotic pressure, allowing the cell to survive. All living cells experience changes in their osmotic environment and therefore must adapt to these changes by several mechanisms. In either case, MS channels are responsible for the release of osmolytes down its concentration gradient in an effort to reduce the turgor pressure applied upon the cell membrane.

*MscL*

The MS channel of large conductance, MscL, has been extensively studied and is well understood. The MscL protein and its gene, *mscL,* were initially identified in *Escherichia coli* in 1994 (*3*). The channel is a homopentamer of 136 amino acid polypeptide chains, each containing two transmembrane domains, TM1 and TM2, joined by a periplasmic loop. The TM1 helices are more hydrophilic in nature and are thus tightly packed in the core of the closed channel complex, whereas the TM2

helices are largely hydrophobic and form the lipid boundary of the protein. Both anions and cations are equally able to pass through the channel pore. Conductance increases linearly with the conductivity of the bath electrolyte. This therefore suggested that the channel pore is quite large (*9*). The hallmark of MscL activation is its exceptionally high unitary conductance, implying a large-scale conformational change.

The original hypothesis of the gating transition of MscL proposed a 10 helix barrel stave model which produced an inappropriately small conductance and small in-plane protein expansion (*10*). The current model for the gating transition exhibits an iris-like 5 helix tilted pore model with a gradual helix expansion and an outward movement of TM helices (*11*). The actual opening transition occurs in two stages, beginning with the expansion of the barrel, followed by the separation of the N-terminal gate. Eventually, upon expansion, the S1 (N-terminal) gate and M1 linkers partially separate, thereby disrupting the S1 bundle and allowing the channel to fully open. Therefore, pore opening is essentially a result of the tilting of both transmembrane helices, with M1 lining the majority of the inner surface. Much support has been gained for this current gating model of MscL.

The N-terminal region is highly conserved in MscL. The most strictly conserved residues are F7 and F10, which are 100% conserved in the EcoMscL subfamily. This region may act as a second gate because it had been thought to act as a pore occluding element to explain the presence of a low conducting sub-state (*12*).

This region is thought to open only after the M1 gate opens and expands upon entering the fully open state.

It has been shown that MscL gating is sensitive to the lipid environment. MscL gates at lower tensions in short chained lipids forming thinner bilayers. It activates in the presence of assymmetrically added amphipathic agents such as lysolecithin (*13;14*). However, because the channel undergoes a large expansion and substantial flattening, the involvement of protein-lipid interactions regarding the channel gating mechanism has not yet been fully resolved.

*MscS*

The MS channel of small conductance, which to date, is much less understood, but has far more abundant homologues than MscL (*15*). MscS is a 286 amino acid protein encoded by the gene *yggB*. The structure of MscS was solved by X-ray crystallography by Bass et al in 2002. It appears to be a homoheptamer with each subunit containing three transmembrane spanning helices denoted as TM1, TM2, and TM3 and a large, cytoplasmic C-terminal domain. TM1 and TM2 in the crystal structure are tilted at ~30° (*16*), but this may be the result of a substitution of the membrane with lipids by detergent in the crystallization samples. The majority of the pore forming TM3 helix is highly conserved and contains a specific sequence of alanine and glycine residues. The specific placement of the glycine and alanine resides allow for the tight packing that is seen in the channel pore.

The original crystal structure of MscS was postulated to represent the open conformation (*16*). Edwards et al assumed the open conformation of the crystal structure and attempted to find a more tightly assembled conformation for the pore lining helices (*4*). However, our computational analyses of the crystal structure have found that the pore is too small to conduct at the experimentally observed level (1nS). The hydrophobic constriction of the pore was found to be largely dehydrated, strongly suggesting that the previously published crystal structure must represent a non conductive state (*17*). Therefore, the helical movements during the gating transition in MscS remain unclear.

MscS has at least three functional states. Closed, open, and the inactivated state. A proposed concerted outward movement of all three helices allows for channel opening and is associated with both dilation and wetting of the pore. The transition from the closed to the fully open state shows a steep dependence on membrane tension. However, the main closed to open transition is essentially voltage independent. At tensions below the activation midpoint, the channel inactivates (*18*). According to the current model, inactivation occurs when the TM3 helices detach from the lipid facing TM1 and TM2 helices and collapse. Additionally, the large cytoplasmic domain, forming a hollow cage-like structure, has been implicated to be involved in the regulation of inactivation of the channel (*19;20*).

*Physiological Approaches to MS Channel Mechanisms*

Bacterial plate counts offer a way to quantify cell survival, allowing us to test the rescuing ability of the channel. It also allows us to see the effects of loss-of-function (LOF) and gain-of-function (GOF) phenotypes. LOF phenotypes are characterized by non-active channels, or channels with an activation threshold that is too high to protect the cell from osmotic down shock. LOF mutations either cause the channel to open at a greater tension or not at all. This phenotype is thus characterized by cell death upon exposure to down shock. Conversely, GOF phenotypes are hyperactive channels with low activation thresholds. Expression either slows down or completely impedes growth. GOF mutants often exhibit constitutive partial activation. Phenotypically, they are characterized by either decreased or poor bacterial growth, especially upon channel induction, essentially due to the leakiness of the channel or an inappropriately low activation threshold (*21*).

*GOF Phenotypes*

The first example of a GOF mutation was generated by Blount et al (*22*). Bacterial cell growth was shown to be slowed by the mutation K31E/D, a charge reversal at the Lysine 31 position in TM1. This demonstrated the importance of the K31-D84 salt bridge in the gating of MscL. IPTG, added to the mutant culture to induce channel expression led to a slowed growth plate and liquid cell culture phenotypes (*23*). In addition to slowed growth, this mutant opened with less tension

in patch clamp experiments, exhibiting a left shift of the activation curve. This particular correlation was vividly illustrated by Ou et al who performed random mutagenesis followed by screens for slowed-growth phenotypes, and Yoshimura et al using site-specific mutations. Random mutagenesis was done in an effort to determine functionally important residues within MscL and it was found that the majority of the GOF residues lie within TM1, suggesting its importance in channel gating. The slowed growth phenotype was caused by solute loss due to an inappropriately low tension threshold in the mutant channels. Polar substitutions at residues G22, V23, G26, and G30 were identified as severe GOF mutations in TM1 located near and at the pore constriction, thus making the pore more hydrophilic.

G22 is buried within the pore constriction of MscL. Yoshimura et al introduced all 19 substitutions for G22 and found that the left-shift of the activation curves and the toxicity of the mutation were directly correlated to the hydrophilicity of the substituted residue (*24*). By doing so, it was found that the insertion of hydrophilic residues decreased the threshold pressure at which the channels opened and also showed an intermediate sub-conducting state. Hydrophobic substitutions were seen to increase the threshold pressure. These results suggested a model for gating where G22 moves from a hydrophobic to a hydrophilic environment upon the transition from the closed to open state. Therefore, since the transition from the closed state to the fully open state requires hydration of the pore, polar substitutions in the constriction decrease the energy gap of the transition with the increasing severity of the mutation (*25*).

*MTS Accessibility*

Accessibility experiments using site directed mutagenesis to generate cysteine mutants allow us to determine the effect in vivo upon the addition of MTS reagents. A hit by MTS at a sensitive site, essentially results in a GOF phenotype. MTS accessibility experiments were studied in the tightly packed pore region, the entire TM3 helix in MscS. The substituted cysteine accessibility method (SCAM) has been used readily to identify exposed residues within a channel pore (*26;27*). This method allows for the binding of sulfhydryl reagents such as MTSET ([2-Trimethylammonium] ethyl Methanethiosulfonate Bromide) and MTSEA ([2-Aminoethyl]methane thiosulfonate Hydrobromide) to cysteine mutants generated in the region. Only those residues which are accessible to the aqueous environment can react and bind. Binding of these reagents to cysteine residues can only occur upon channel opening, resulting in a variety of effects relating to both cell survival and gating kinetics. If the channel pore is quite small, this binding upon channel opening often results in a decrease in conductance.

These findings were emphasized with the use of methanethiosulfonate (MTS) reagents binding to G22C as discussed below. Studies were done through patch clamp experiments with differently charged groups bound to MTS. Because there are no native cysteines in wild-type MscL, this single amino acid change allows for the binding of a sulfhydryl group on each of the five identical subunits that form the channel. MTS reagents vary in length as well as hydrophobicity and are specifically reactive to sulfhydryl groups and have been used to chemically modify such groups if

they are accessible. The effect of charged substitution can be mimicked by the addition of MTS reagents with differing polarity. It was thus concluded that hydrophilicity inside the gate region correlates with the mechanosensitivity of MscL.

Batiza et al used SCAM to study MscL substituting cysteine mutants in the TM1 region to test for accessibility *in vivo* (*28*). A charged thiosulfonate reagent $MTSET^+$ was attached to residue L19, made accessible by the application of sufficient down shock, thereby creating a toxic GOF channel. Thus, channel opening can be manifested by loss of colony forming units. In addition, L19 opened by suction in the presence of $MTSET^+$ in voltage-clamped patches, showed spontaneous openings. These observations showed that MscL opening was triggered by down shock and that residue 19 becomes exposed upon channel opening. It was also confirmed that residue 19 is inaccessible in the closed state.

*LOF Mutations and Second-site Suppressors of GOF Mutations*

Loss of function phenotypes are characterized by a loss of ability to rescue the channel upon down shock, typically associated with right shifts of activation pressure. The random library generated by Maurer and Dougherty for MscL showed a large pattern of LOF sites at both the protein-lipid interface and in the loop region (*7*). This points to very critical residues in these regions. Areas of residues not critical to channel function will generally not exhibit LOF of GOF phenotypes and will essentially be like WT. Additionally, random mutagenesis and phenotypic screens were designed to look for second site suppressor mutations that restore toxic

substitutions. Li et al attempted to search for such mutations to restore V23A and G26A, two toxic GOF mutations (*29*). There was one GOF suppressing mutation that was shown to be found in the S1 domain, allowing for some speculation that the S1 domain is involved in the gating mechanism.

Rightward shifts of the midpoint of activation cause LOF phenotypes, decreasing the rescuing ability of a channel under hypotonic shock conditions. However, certain types of GOF mutations can lead to a LOF effect. This in part can occur when a particular mutation causes a leak in the gate (GOF) for structural reasons but disrupts the opening process, also giving a LOF effect. Mutants can undergo a second mutation that restores the original phenotype. If a mutation at a different site restores the original phenotype it is a second-site suppressor mutation. This type of intragenic suppression occurs at a different site and restores the function of the protein and is often used to study the interactions of residues within a protein, such as between two domains.

Yoshimura et al (*30*) attempted to randomly generate second-site suppressors for a GOF mutant, G22D. This resulted in a small set of mutations at the lipid boundary and the periplasmic loops of MscL, where many LOF mutations were previously identified. An effort was made to explore the protein-lipid interactions between these two areas by asparagine scanning mutagenesis. It was found that seven of these mutations were effective in reducing the tension sensitivity of the channel, emphasizing the importance of protein-lipid interactions.

Li et al also studied intragenic site-suppression through random mutagenesis and growth selection of the V23A and G26S mutations. An alternative approach to isolating LOF mutants is to generate intragenic suppressors of GOF mutants (*29*). The suppressor mutants were characterized by growth phenotype, western blot and patch clamp techniques. A correlation was found between the severity of the phenotype and an increase in sensitivity of the channel activity to membrane tension. intragenic mutations were identified that suppress two of the most severe GOF mutants, V23A and G26S. Intragenic suppressing mutations may give clues to interactions that may occur upon channel gating. It was found that the majority of the second-site intragenic mutations suppressed the GOF phenotype by an overall depression of channel activity, most likely by leading to slight LOF phenotypes with higher energy requirements for gating. These mutants clearly demonstrate the importance of protein-lipid interactions, leading to the gating transition (*7*).

*Rationale for further Investigation*

Cells that lack both MscS and MscL or cells which only contain the empty vector are not able to rescue the channel upon sufficient down shock (*2*). Because the channels are partially redundant, to test MscL or MscS we must use cells which lack both channels. Therefore, through the generation of various mutants we can test their rescuing ability by stimulating them either by osmotic down shock or by tension applied to the membrane in patch clamp experiments. The majority of the work will

be quantified through plate counts which when compared to the control, allow us to see the result of MS activation.

The present work focuses on the studies of protein-lipid interactions through aromatic substitutions in lipid facing helices of MscL. There is a conspicuous absence of aromatic caps, native to many membrane proteins, in MscL. This absence of aromatic anchors is vital for channel function due to the strong reorientation of the TM1 and TM2 helices. Data shown below demonstrates that capping the helices with aromatic residues affects the opening transition, as this transition is predicted to be associated with a strong helical reorientation. Restraining helical positions in MscL by introducing specific protein-lipid interactions at membrane interfaces compromises MscL function. We examine how the rescuing function *in vivo* and the gating parameters of MscL in electrophysiological experiments depends on the presence and specific positions of aromatic anchors at the ends of transmembrane helices. We have performed hypotonic shock experiments to evaluate the ability of mutants to rescue *mscL-, mscS-* cells from osmotic lysis compared to WT MscL. And in parallel, patch clamp experiments used to characterize the energetic and kinetic properties of mutant channels.

In MscS, which is far less understood, contradictory interpretations of the crystal structure exist. Thus, there is a strong need to experimentally verify the existing models of the open conformations of MscS generated by MD simulations in our laboratory, by studying the dynamics and accessibility of TM3 helices both in the resting state and during the gating transition. In studies of the gating transition of

MscS, we have examined not only the constriction region, but also conducted an entire scan of the TM3 helix, replacing residues within the gating region with cysteine residues to allow us to perform accessibility experiments as well as cell viability assays with MTS reagents, primarily MTSET.

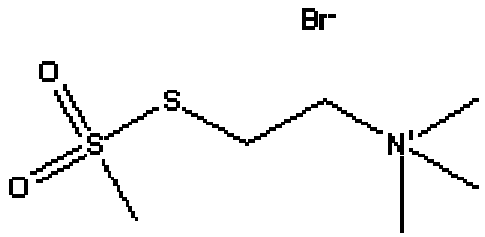


Because chemical modifications of grafted cysteines with MTS reagents often result in strong gain of function (GOF) phenotypes, the accessibility of certain residues in different functional states can be tested (*26;31*). Other experiments with MscS involve an attempt to move the gate by first one turn up, and time permitting, two turns up.

# Chapter 2: Materials and Methods

## *Strains and Molecular Modifications*

The megaprimer technique was primarily used to generate mutants for MscL and the Quick-change kit (Stratagene) was used for the generation of the MscS mutants. For the megaprimer technique, two rounds of mutagenic PCR with Pfu polymerase (Stratagene) were performed with the wild type MscL ORF (plasmid p522b) as the template. The amplified mutant ORFs were gel purified, digested with Bgl II and Xho I and cloned into the pB10b vector, behind the $P_{lacUV5}$ inducible promoter. This procedure was then followed by automated DNA sequencing to confirm the validity of the clone.

### *MscL*

Single aromatic substitutions I41W, Y75F, I79W, F93Y, F93W, L98W, L102W, L102Y, two double substitutions Y75F/F93Y and I79W/F93W, and a charge substitution Y75E were all introduced for the aromatic cap studies with MscL. All constructs and WT MscL are cloned into the pB10b vector and transformed into MJF455 *mscS-, mscL-*, cells kindly provided by Dr. Ian Booth (University of Aberdeen, UK) for hypo-osmotic shock experiments. For patch clamp experiments,

the mutants are to be expressed in PB104(ΔΩ3a) *mscS+, mscL-* cells where intact MscS can be used as an internal tension gauge for patch clamp characterization.

*MscS*

For the gate region of MscS 12 mutations were made. For studies involving the cysteine scan of the TM3 helix, 10 mutations were made which include, A98C, V99C, L100C, G101C, A102C, A103C, G104C, A106C, V107C, and G108C. MscS mutants were expressed into MJF465 cells which are *mscL-, mscS-,* and *kefA*-, lacking all MS ion channels making it a prime choice for cell viability assays. The A102L/L109A and A102V/L109A mutants were also generated in an attempt to move the pore constriction up one helical turn.

<u>*Control of Protein Expression*</u>

*MscL*

One-mL samples of induced and non-induced cultures at $OD_{650}$ of 0.6 ($6.7\times10^8$ cells/ml or 85 μg/ml dry weight) was be prepared for osmotic survival tests and withdrawn before harvesting for Westerns. Cells for both MscL and MscS were French-pressed and the membranes collected by centrifugation at 17,000 g for 35 min. The membrane pellet was dissolved in 50 mL of 2x SDS sample buffer and heated to 60$^o$C for 10 min. The volume of samples per well applied to the gel was

20 µl for uninduced cultures and 8 µl for induced. Membrane proteins were resolved on SDS gels, electroblotted on PVDF Immobilon membranes, and the MscL and MscS band, separately for two experiments were visualized with primary antibodies raised against the N-terminus and AP-conjugated secondary antibodies for MscL and with commercially available AP-conjugated anti-6-His antibodies for MscS.

*MscS*

Both strips of PVDF membrane containing induced and non-induced samples were incubated with antibodies, washed and developed with Western Blue stabilized alkaline phosphatase substrate (Promega) in the same tray under identical conditions. Digital images of membranes were taken under transillumination on an Alpha Imager (Alpha Innotech, San Leandro, CA) and the amounts of color in the bands were subjected to digital densitometry. The background color density distribution in the PVDF membrane was reconstructed based on values of protein-free areas outside the bands and subtracted from values within the bands using custom-written program GELAN (A. Anishkin).

*Electrophysiology*

For patch-clamp experiments, the mutants were expressed in PB104 cells for MscL and MJF465 cells for MscS, both involving the preparation of giant spheroplasts (*32*). Intact MscS channel present in PB104 cells activates at 5.5

dynes/cm and can be used as an internal tension gauge to convert pressure into the scale of tension which can then be analyzed using PClamp 8 software (Axon Instruments). Most electrophysiological analysis has been performed by Dr. Chien-Sung Chiang and Dr. Sergei Sukharev. Patch clamp methods were used to study channels from giant spheroplasts. Channels were stimulated by suction applied to the pipette, thereby generating membrane tension. Recordings were taken in excised patches in the voltage clamp mode using an Axon 200B amplifier and a DigiData 1320A A/D converter (Axon Instruments). Electrodes were made of borosilicate capillaries and pulled to a bubble number of 4.5 on a micropipette puller (P-97 Sutter Instruments). Recordings for MscS were performed in symmetrical potassium buffers in the pipette (200mM KCl, 90mM $MgCl_2$, 10mM $CaCl_2$, 10mM HEPES pH 7.2).

*Cell Viability Assays*

Overnight cultures of cells carrying one of the expression vectors was grown in LB media in the presence of 100µg/mL ampicillin. 1mL of the overnight cultures were transferred into 20mL LB supplemented with 0.5M NaCl (Hi LB, 910 mOsM) and grown to an $OD_{650}$ of 0.6 for non induced experiments. In experiments with induced cultures, cells were grown to and $OD_{650}$ of 0.3, and induced with 0.8mM IPTG and grown a further 25 minutes to reach an $OD_{650}$ of 0.6 (+/- 0.02). After the period of induction, 500µl of each culture was transferred into a culture tube containing 5mL of Hi LB (control) and 5mL of LB diluted two times with de-ionized water (LB/2), 200mOsM) and left at room temperature for 15 minutes. The cell

samples were then diluted $10^{-3}$ and $10^{-4}$ times with the same shock medium (LB/2) and plated in duplicates on standard LB plates. For survival controls, the HiLB-adapted cultures were transferred into 5mL of HiLB, diluted, and plated in duplicates on standard LB plates. The following day involved manual colony counts with both the mean and standard errors determined

*MTS Accessibility Experiments*

These assays begin similarly with overnight cultures and growth in HiLB to an $OD_{600}$ of about 0.3 and induced with 0.8mM IPTG and grown a further 20 minutes to reach an $OD_{600}$ of 0.6 (+/- 0.02). After induction, cells were harvested and resuspended in and iso-osmotic sodium phosphate buffer. Shock experiments were conducted with two buffers of sufficient osmolarity to allow for a WT survival of about 85%. Buffer solutions must be used in order to eliminate binding of MTS reagents to free cysteines present in bacterial growth media. Otherwise, cell viability assays are conducted as above with the addition of 0.6mM MTSET to the shock and control tubes and plated as before in duplicates. MTS reagents were diluted into water since the half life in buffer was listed as only 11 minutes. This data will be compared to assays in the same buffer media without the presence of MTSET with manual colony counts the following day.

*Growth Curves*

In order to assay for LOF or GOF phenotypes and to be sure none of the cell death or slow growth is a result of the these phenotypes, growth curves must be carefully measured in order to determine if there is any variation from WT. A GOF mutant is expected to grow to a lower density. This is essential to verify whether or not cell death is due to a loss of function phenotype since there are other factors which contribute to cell death upon amino acid substitutions within the channel genes. Overnight cultures were prepared from freshly streaked agar plates supplemented with 100ug/ml of ampicillin. The cultures are then grown at 37° C shaking at 255 rpm for 6-8 hours until growth saturation is reached. After one hour and 30 minutes the cultures are induced with 0.8mM IPTG. Optical density was measured and recorded every 30 minutes at an $OD_{600}$ until saturation. No such phenotypes were found according to growth parameters.

# Chapter 3: Capping of MscL Helices

*Problem Statement*

The crystal structure of the MscL homolog from *M. tuberculosis* (TbMscL) in its closed conformation was determined to a 3.5 Å resolution *(5;33)*, revealing a homopentameric assembly of two-transmembrane domain subunits. The TM1 helices, more hydrophilic in nature, are tightly packed in the core of the closed channel complex, whereas the largely hydrophobic TM2 helices form most of the lipid-facing boundary of the protein. To relate ample functional data collected mostly on the *E. coli* channel, a homology model of EcoMscL derived from the TbMscL crystal structure was subsequently proposed and analyzed *(11;12)*.

The hallmark of MscL activation is its exceptionally high unitary conductance (~3 nS in 350 mM salt) implying a large-scale conformational change. Using the crystal structure as well as the EcoMscL homology model as initial conformations, several possible pathways for the opening transition were inferred (*10*). The initial hypothesis was that under membrane tension the cytoplasmic ends of TM1 domains move apart and TM2 helices wedge between TM1s forming a barrel-like aqueous pore made of almost parallel helices-staves *(34)*. An alternative model of the open state suggested a concerted tilting of TM1-TM2 pairs associated with a simultaneous outward movement in an iris-like manner. The latter model received experimental support by cysteine cross-linking (*31*) and EPR experiments *(35)*. The predicted tilting of TM1-TM2 helical pairs by about $35^{o}$ produces a 3 nm-wide pore and leads to a substantial shortening of the channel barrel. This flattened conformation was

expected to produce a thickness mismatch with the surrounding lipids, which was supported by the reduced pressure thresholds for MscL channels reconstituted in lipid bilayers made of shorter chain lipids (*30*). In addition to the thickness of the hydrocarbon layer, the chemical nature of lipid headgroups and related lateral pressure profiles in the surrounding bilayer were found to be important determinants for the energetics of gating *(21)*.

Chemical heterogeneity of lipid bilayers in the transversal direction produces another level of complexity in protein-lipid interactions. Structural analysis of a large variety of membrane proteins have indicated that aromatic residues Tyr and Trp are enriched at the ends of TM helices, having specific affinity for the region near the polar/apolar interface of the membrane, coinciding with the region of phospholipid carbonyls. These residues were proposed to anchor the ends of TM segments to the membrane interface and thereby stabilize the protein structure. The distribution of amino acids in the transmembrane domains and flanking regions in MscL proteins from 35 bacterial species was found to be non-random (*21;36*). Phenylalanines frequently occur in all 35 MscL homologs, preferentially in the second transmembrane domains (TM2) facing the lipid. Tyrosines or tryptophans, in contrast, occur infrequently in the helixes and never on both ends. EcoMscL and other species from the same sub-family has only one Tyr located at the periplasmic end of TM2 (Y75 of EcoMscL) while representatives of the more distant mycobacterial subfamily typically have two tyrosines, both at the cytoplasmic side of TM2 (Y87 and Y94 in TbMscL).

Here we examine how the osmotic rescuing function *in vivo* and gating parameters of MscL in electrophysiological experiments depend on the presence and specific positions of aromatic anchors at the ends of transmembrane helices. We perform hypotonic shock experiments to evaluate the ability of mutants to rescue *mscL*$^-$, *mscS*$^-$ cells from osmotic lysis and compare it with wild-type MscL. In parallel, we use patch-clamp recording in giant spheroplasts to characterize the energetic and kinetic properties of the mutant channels.

For analysis of LOF mutations, wild-type strains may not be suitable. For instance, single knock-outs carrying deletions of either *mscL* or *mscS* genes would be unsuitable for osmotic-shock survival screens since the two genes are functionally redundant the single mutants do not possess any osmotic fragility phenotype. The analysis of redundancy and preparation of double knock-outs previously accomplished by the Booth laboratory (*2*) resulted in strains that do not survive osmotic down shocks larger than 400 mOsM in magnitude that can be rescued by re-expression of either of the functional proteins.

The iris-like mechanism of MscL is illustrated in Fig.2. It has been shown previously that in order to satisfy the measured unitary conductance, the transmembrane barrel has to expand by 20-23 $nm^2$ producing a water-filled pore of 3 nm in diameter (*35*).

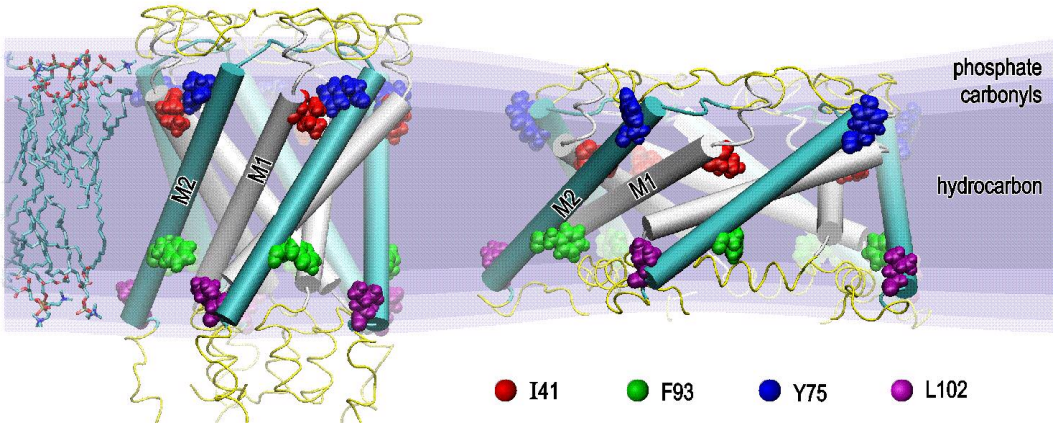


**Figure 2**. Models of the EcoMscL transmembrane barrel in the closed and open states. Opening of a 3 nm water-filled pore is associated with the increase of TM1 tilt from ~30$^{o}$ to ~65$^{o}$ relative to the membrane normal. The positions of alpha carbons on lipid-facing helices are shown as hemispheres and the residues targeted by mutations are numbered. The models are aligned with the layered distribution of chemical groups in the simulated POPC bilayer (shown on the left). Since the open conformation of the barrel is substantially flattened, a hypothetical thinning of the bilayer around the protein can be expected. Capping of both ends of the TM2 helices with aromatic residues is predicted to restrain their ability to tilt.

This conformation with TM1 helices tilted at 65-70$^{o}$ to the pore axis was previously supported by the A20C-L36C crosslink (between two adjacent TM1), also shown to stabilize the open state of the channel. Another bridge, I32C-N81C, linking TM1 and TM2 of two subunits permitted channel gating thus suggesting that adjacent TM1 and TM2 do not change their relative positions substantially during opening and thus should tilt together. This pairing of helices predicts a strong tilt for TM2 as well, and must produce a substantial flattening of the helical scaffold of the barrel. The figure illustrates the positions of several lipid-facing residues relative to the layered distribution of chemical groups in the surrounding bilayer, upon which the models of the closed and open states are superimposed. Because the flattened open conformation is expected to distort boundary lipids, a thinning of the bilayer is

expected. The figure is highly schematic and represents only the predicted spatial scale of helical rearrangements in a typical bilayer, but does not take into account the actual conformations of the boundary lipids and side chains in this anisotropic environment.

The scheme shows that in the tightly packed closed state, the distribution of aliphatic and aromatic residues generally corresponds to the hydrocarbon core and the adjacent layers of carbonyls/glycerols. On the outer surface, Y75 lies just at the level of carbonyls and I41 on TM1 probably faces the nearby hydrocarbon. On the inner surface, it is likely that F93 (homologous to Y87 in TbMscL) also resides at the hydrocarbon boundary or in the carbonyl/glycerol layer. L98 situates amid carbonyls and glycerols, and L102 likely extends into the level of phosphate groups, although it is hard to predict the exact conformation of its side chain. When MscL opens, TM1 helices are predicted to tilt more than TM2. We presume that in the open state Y75 stays in its most favorable environment, the carbonyl/glycerol layer, while tilting of the helices submerges their opposite (cytoplasmic) ends deeper into the hydrocarbon, posing no apparent hydrophobic conflict. From the scheme it is easy to see that aromatic (Y or W) substitutions for F93 and L98 at the end of TM2 stabilizes more upright positions of helices (closed state) as tryptophans and especially tyrosines have higher affinities to this anisotropic boundary layer of intermediate polarity. Tilting may require either a costly repositioning of these aromatic anchors from the carbonyl-occupied zone or stronger distortion of the boundary lipids. The presence of aromatic anchors on one side, and never on both ends of the lipid-facing helices in all known MscL homologs may serve its purpose. The experiments below are designed to

answer the questions of what would happen if the aromatic anchors in EcoMscL were moved to the cytoplasmic side of TM2, as they are in mycobacterial MscLs, and what would be the effect of having aromatic anchors on both ends of the helixes.

## *Results*

Among the mutations introduced in the lipid-facing TM2 helix, Y75F removes the canonic aromatic anchor, and Y75E replaces it with a negatively charged cap. The double Y75F/F93Y mutation moves tyrosine from the periplasmic to the cytoplasmic end of TM2. When introduced on the wild-type background, mutations F93Y, F93W, L98W, L102Y, L102W add the second aromatic cap on the cytoplasmic side, at different distances from the existing extracellular cap (Y75). The I79W mutation adds the second anchor to the periplasmic end of M2 one helical pitch below Y75, whereas double I79W/F93W has two aromatic residues on the periplasmic side and one on the cytoplasmic side. Additionally, the I41W mutation introducing an aromatic cap on the extracellular end of TM1 was generated.

### *Protein Expression and Osmotic Survival Assays*

WT and all mutants were expressed in MJF455 (*mscL-, mscS-*) bacteria and tested for their rescuing ability against a 700 mOsM osmotic down shock. Bacteria were pre-grown in the high-osmotic medium (HiLB, 900 mOsM), diluted into low-osmotic medium (LB/2, 200 mOsM) and plated after several serial dilutions. The

magnitude of osmotic downshift (700 mOsM) was adjusted to inactivate almost 100% of the control MJF455 cells carrying empty vector, but to retain a 40-50% survival when WT MscL is expressed at a low level. High levels of WT MscL expression resulted in 95% survival. The procedure was repeated at least 3 times for each mutant, with both induced and non-induced cultures.

Prior to osmotic shock, one milliliter of each culture was sampled and the MscL protein content was quantified using Western blots. As shown in Fig. 3A, all mutant proteins were produced at a fairly uniform level, comparable to WT MscL. Even without induction, an appreciable amount of channel proteins is produced through the $p_{lacUV5}$ promoter 'leakage'. This amount corresponds to 3-5 channels per patch sampled with standard 0.5 μm pipettes *(25)*.

The densitometry indicated that the total amount of color associated with each protein band increases 3-14 (5.5 times in average) upon induction of the $p_{lacUV}$ promoter with 0.8 mM IPTG. Given the difference in gel loading (2.5 times larger sample volume for non-induced samples), the total increase in protein expression level is 14 fold in average, consistent with the number of channels per patch found in induced and non-induced spheroplast preparations ( Table 1).

| MscL mutant | Number of channels per patch, un-induced /induced | Open dwell time (ms) | | | Activation midpoint, $\gamma_{1/2}$ (dyne/cm) | Relative survival upon osmotic down shock | |
|---|---|---|---|---|---|---|---|
| | | τ1 | τ2 | τ3 | | Un-induced | Induced |
| WT (Y75) | 5/50 | 0.1±0.1 | 6.2 ± 1.5 | 21±4.0 | 10.2±0.6 | 1.00±0.14 | 1.00±0.1 |
| Y75F | 6/45 | 1.7±1.4 | 12±2.3 | 24±4.0 | 10.3±1.1 | 0.73±0.26 | 0.95 ±0.05 |
| Y75F/ F93Y | 4/60 | 1.5 | 28.3 | 213 | 13.5±0.6** | 0.28±0.01 | 1.1±0.05 |
| F93Y | 6/60 | 0.3±0.2 | 25±9.7 | 80±22 | 13.0±0.7** | 0.42±0.20 | 0.91±0.1 |
| F93W | 5/60 | 0.2±0.1 | 29±18 | 360±24 | 13.2±0.8** | 0.32±0.05 | 0.88±0.2 |
| L98W | na/55 | < 0.1 | 7.2±4.1 | 26±5.6 | 13.2±0.3** | 0.47±0.17 | 0.28±0.1 |
| L102Y | 6/70 | 0.8±0.7 | 35±17 | 91±20 | 11.6±0.6* | 0.60±0.09 | 0.71±0.1 |
| L102W | 5/60 | 2.3±0.9 | 28.0±20.5 | 90±3 | 11.5±0.9* | 0.4±0.13 | 0.88±0.12 |
| I79W | 4/50 | < 0.1 | 1.3±0.1 | 8±2.0 | 11.2±0.5* | 0.18±0.02 | 0.42±0.1 |
| Y75E | na/32 | 0.7 | 29.3 | 190 | 11.4±0.9* | 0.02±0.01 | 0.04±0.004 |
| I41W | na/10 | 0.6±0.2 | 2.2±0.4 | 7.0±3.0 | 8.4±0.7** | 0.08±0.06 | 0.04±0.01 |

**Table 1**. Electrophysiological properties of mutants and osmotic survival in comparison with WT MscL. The percentage of cell survival for each mutant is normalized to the survival of WT under identical conditions. According to t-test, the midpoint tension ($\gamma_{1/2}$) for mutants was statistically different from that of WT with P<0.05 (*) or P<0.001 (**). Relative survival is presented as the mean ± standard error.

Somewhat lower levels of the I41W protein was observed under non-inducing conditions, but with induction, the density of the corresponding band was comparable to WT and other mutants. None of the mutants exhibited a toxic 'gain-of-function' phenotype *(34)*, no growth retardation was observed on plates, or in liquid cultures of regular or HiLB.

Fig. 3B presents cell survival upon a 700 mOsM osmotic down shock for each of the mutants and cumulative Table 1 compares survival with the electrophysiological properties of the channels. All substitutions compromise the rescuing function of MscL to a different degree. A removal of the conserved extracellular aromatic cap (characteristic for the EcoMscL subfamily) through the Y75F substitution led to insignificant differences in survival under induced conditions and only a mild decrease under low-copy expression, compared to WT. Moving the aromatic cap from the periplasmic to the cytoplasmic side (Y75F/F93Y) led to a significant decrease in survival in uninduced cultures, but essentially no change in induced cultures. Addition of the second aromatic cap at position 93 (F93Y or F93W) reduces survival only in uninduced cultures. Extending the distance between the caps along the helix in the L98W or L102Y/W mutants show tendencies to improve survival under low-copy conditions, but for some reason this did not correlate with the survival under full induction for L98W.

The second aromatic cap at the periplasmic side (I79W) or in combination with a cytoplasmic cap (I79W/F93W) strongly compromises channel performance under both induced and non-induced conditions. Y75E or I41W result in a complete loss of function, in both uninduced and induced cultures. Based on the densities of bands on the Western blot (panel A), this drastic decrease of viability cannot be explained by low expression of these proteins. The magnitudes of changes illustrate that low-copy expression conditions better resolve subtle differences between the mutants. Performing survival tests with full induction masks subtle differences in mild mutants, but confidently reveals severe loss of function phenotypes.

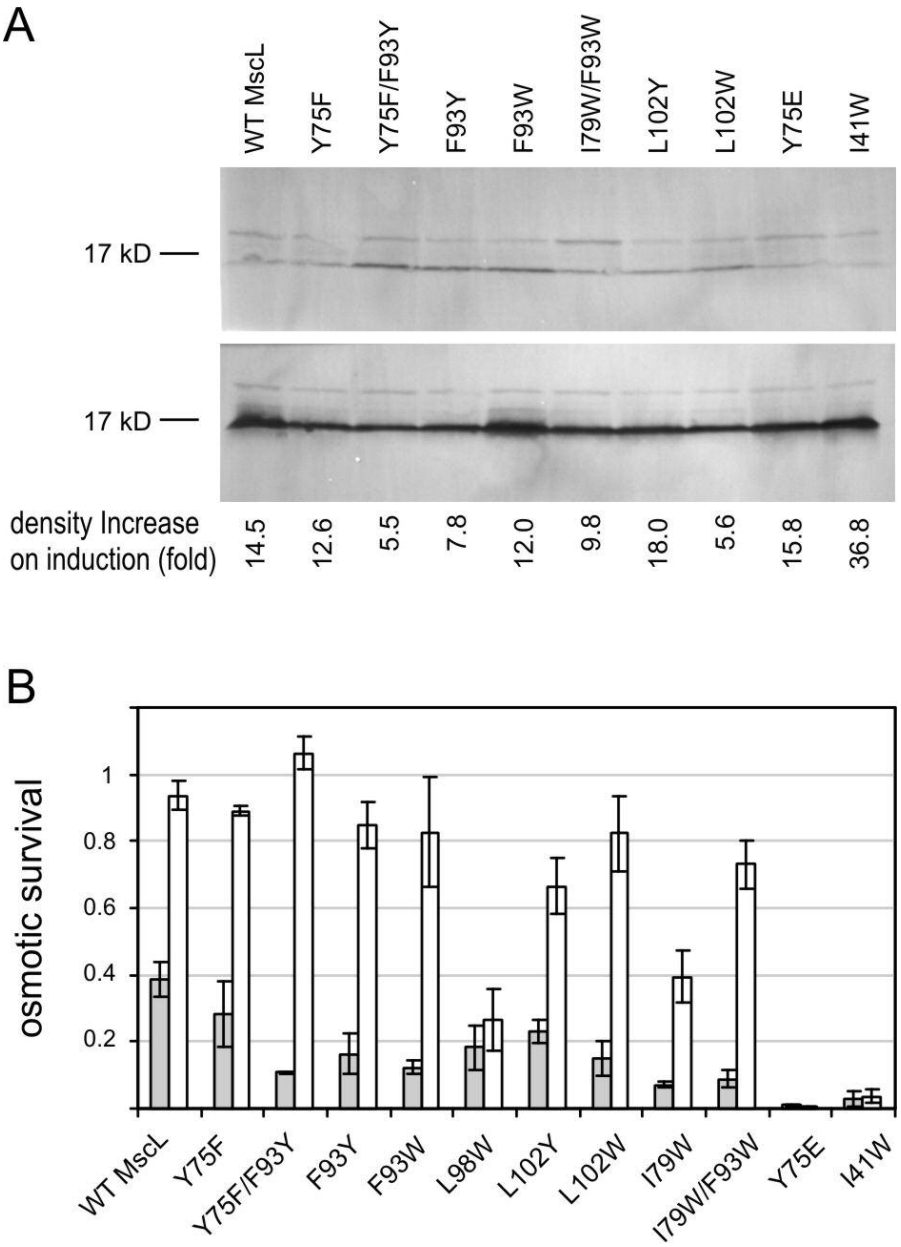


**Figure 3**. Expression levels of mutant proteins and osmotic survival of MJF455 bacteria under non-inducing and inducing conditions. (A) Western blots of membrane samples developed with anti-MscL antibodies without (top) and with 25 min induction by IPTG (bottom). The fold for total density associated with the band is indicated. (B) Survival of MJF455 cells expressing different MscL mutants upon a 700 mOsM osmotic downshift. Induced cultures (white bars) express more channel protein and their survival appears to be less sensitive to mutations. The survival of severe loss-of-function mutants Y75E and I41W is low and independent on the level of expression.

*Channel Gating Parameters*

All studied mutants formed channels that could be activated with suction under standard patch clamp conditions. The measurements were performed uniformly in giant spheroplast preparations (*37*), both induced and non-induced, and the cumulative data are presented in Table 1. Segments of traces illustrating typical gating patterns are shown in Fig. 4, whereas the dose-response (activation) curves and kinetic characteristics of mutants most drastically deviating from WT are illustrated in Fig. 5. To illustrate the correlation between relative changes in rescuing channel ability with changes in gating parameters, the osmotic survival is plotted against the activating tension ($\gamma_{1/2}$) and the predominant open dwell time in Fig. 6. Consistent with the survival data, Y75F showed no strong deviation from WT either in mean open time, or in activation midpoint. The double Y75F/F93Y mutants produced extremely long openings and a right shift of the activation curve, with the midpoint tension increased by 3 dynes/cm (~30%). The F93Y substitution by itself also increases open dwell time, but less than the double mutant, although the right shifts of activation in both mutants are comparable, which correlates with the reduction in shock survival. F93W is also 'stiff' and sets the record for the mean open time duration, which is prolonged to about 0.4 s, i.e. about 20 times the WT at a comparable Po near $10^{-2}$ (Fig. 4).

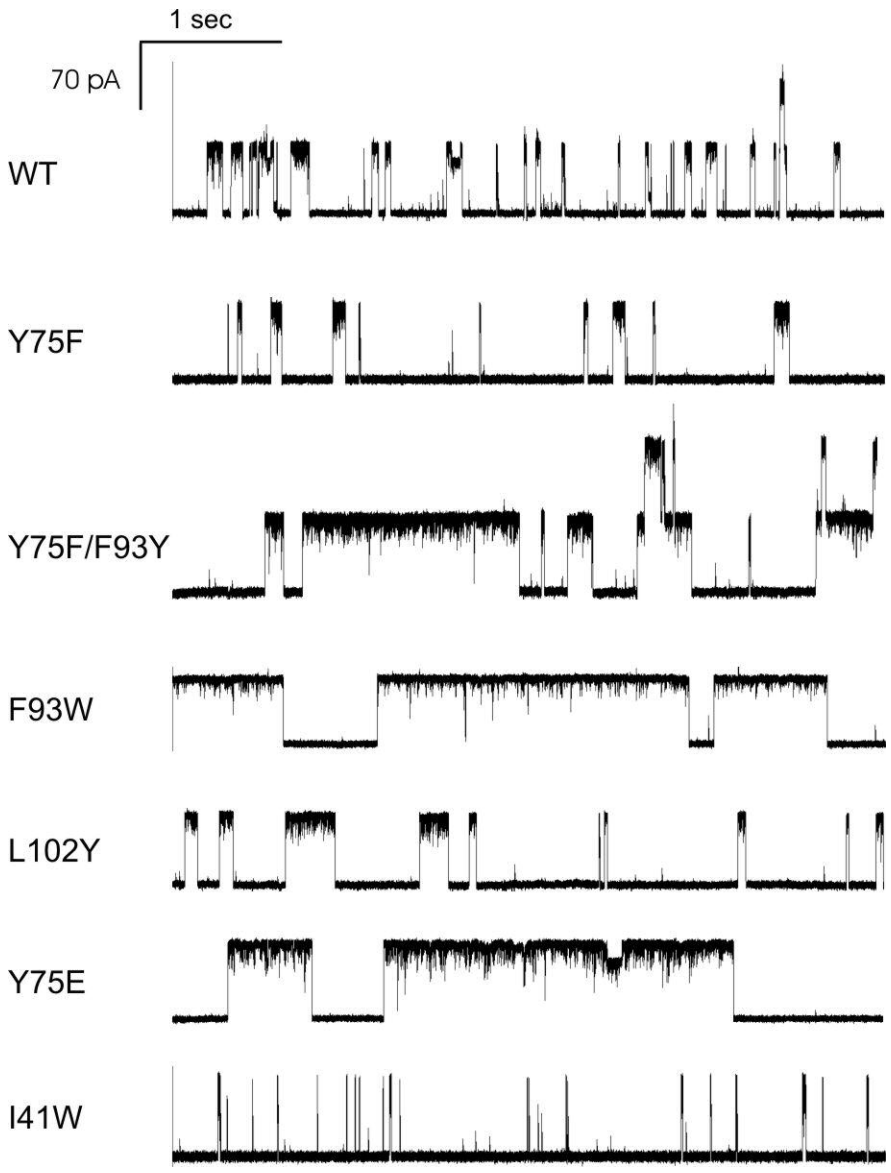


**Figure 4**. Characteristic fragments of single-channel traces recorded from giant spheroplasts expressing mutant MscLs on the *mscL*-null background (strain PB104). Currents were measured from excised inside-out patches at -20 mV under symmetrical electrolyte conditions (200 mM KCl, 10 mM $CaCl_2$, 90 mM $MgCl_2$, 5 mM Hepes-KOH, pH 6.0). The magnitude of pressure gradients (200-300 mm Hg) was chosen such that predominantly one channel was active at a time, out of 20-50 channels present in the patch, being open at Po between $10^{-2}$ to $10^{-2}$ (induced spheroplasts).

The dose-response curves for F93W, F93Y and I41W and dwell time distributions are compared with WT in Fig. 5. L98W, placing a tryptophan about one helical turn below F93, exhibits the same 30% shift in activating tension, but in contrast to substitutions at position 93, has an open dwell time very close to that of WT. These differences to substitutions in position 93 may be caused by different axial and angular positions of the residue in the helix. The Y or W substitutions at position L102, both exhibited slightly longer open dwell times and slightly higher activating pressures, but was essentially indistinguishable.

Introduction of the second aromatic residue at the periplasmic end (I79W) caused a slight right shift of activation, but reduced the mean open time and osmotic survival. The charged cap Y75E introduced instead of the aromatic cap made the channel 'stiffer' and extended the mean open time dramatically. Introduction of an aromatic cap in TM1 (I41W) markedly decreased the tension midpoint and open dwell time. The two latter mutations, as shown above (compare Figures 3B and 6), completely suppress the rescuing ability of MscL *in vivo* independently on the level of protein expression.

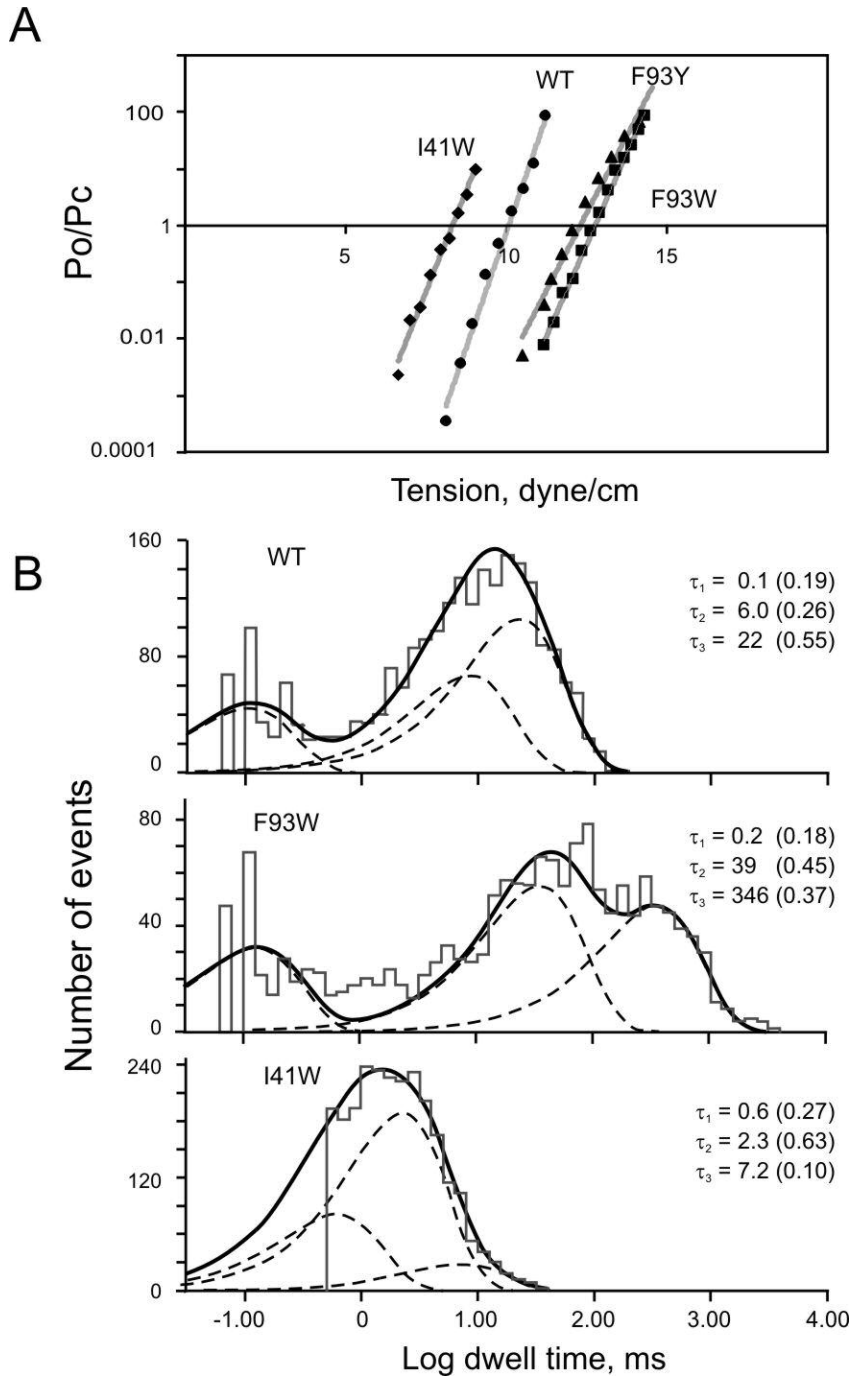


**Figure 5**. Single-channel characteristics of selected mutants which deviate drastically from WT. (A) Representative activation curves for WT, I41W, F93Y and F93W MscL plotted as log(Po/Pc) versus membrane tension. The conversion of pressure to tension scale was achieved by using the MscS activation midpoint as a reference point ($\gamma_{1/2}^{MscS}$ = 5.5 dyne/cm) (11). All curves were fit with a two-

state Boltzmann model. The ratio of open and closed probabilities Po/Pc = exp[–(ΔE–γΔA)/kT], where ΔE is the energy of the opening transition in an unperturbed membrane, ΔA is the protein in-plane area change and γ is membrane tension. The midpoint, $\gamma_{1/2}$, is the intercept with the horizontal axis, where Po=Pc, and correspondingly the energy can be related to the midpoint tension as $\Delta E = \gamma_{1/2}\Delta A$. The midpoint tension shows a leftward shift in I41W while displaying a rightward shift in F93W and F93Y. (B) Open time distributions for WT, F93W and I41W MscLs fitted with three exponents. The characteristic times are denoted as $\tau_1$, $\tau_2$ and $\tau_3$ with relative contributions in parenthesis. The traces were recorded at $P_o$ between $10^{-3}$ and $10^{-2}$. Note that F93W exhibits longer open times, while I41W significantly shorter open times than WT. The cumulative data for all mutants is presented in Table 1.

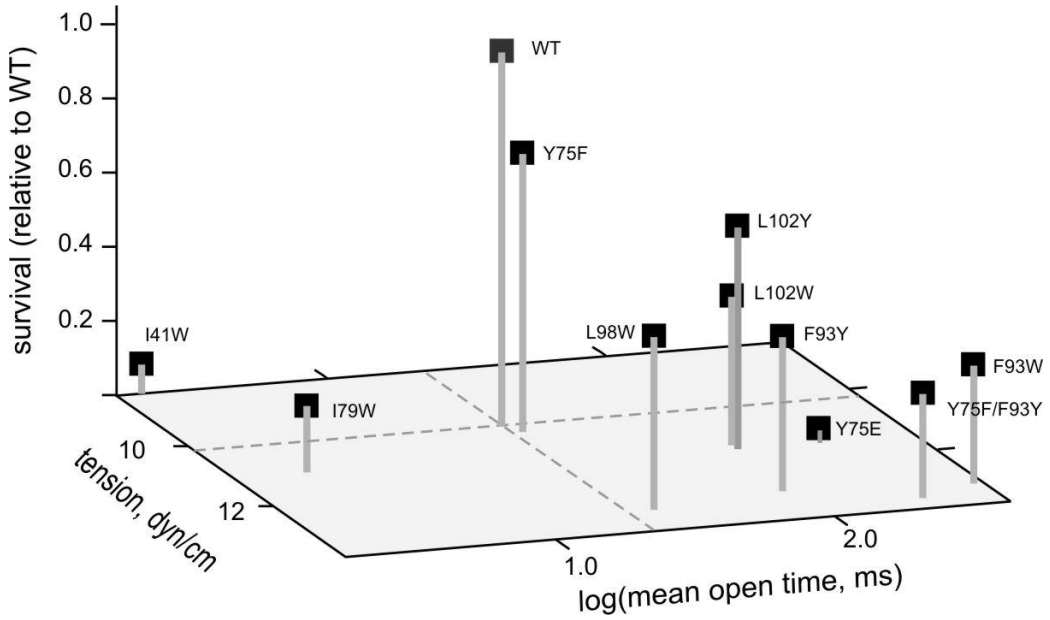


**Figure 6**. Survival of mutants under low-copy (uninduced) conditions plotted as a function of gating parameters, midpoint tension ($\gamma_{1/2}$) and mean open time. For mutants with drastically different kinetics (such as I41W, F93W) the most represented dwell times were taken in consideration. It is evident that deviation in any direction from WT parameters (indicated on the tension-dwell time plane by dashed lines) compromises the rescuing ability of the channel.

*Discussion*

Tension is transmitted to MscL through the lipid bilayer, thus making protein-lipid interactions critical for channel function. Previous studies indicated that the lipid chain length, an asymmetrically imposed positive curvature stress (*14*) or the headgroup composition (*36*) drastically affect tension thresholds for MscL activation. Conversely, hydrophilic substitutions on the lipid-facing surfaces of MscL perturb protein-lipid interactions and reduce the channel sensitivity to tension, leading to loss-of-function phenotypes (*21;35*). The data presented above shows that even more subtle alterations in the lipid-facing surface of MscL via repositioning of aromatic residues can also change the gating energetics. Tyrosines and especially tryptophans are known to interact more specifically with the layer of carbonyls/glycerols than the less polar phenylalanines. TbMscL, when expressed in *E. coli*, displays an extremely 'stiff' phenotype and fails to rescue cells from osmotic shock (*30*), thus the evolutionary conservancy of different tyrosine positions in the EcoMscL and TbMscL subfamilies is mysterious and needs to be explained. It is possible that the anchoring of the protein to the lipid bilayer in the two divergent groups of bacteria was optimized to the specific lipid composition and/or character of membrane asymmetry. The two channel proteins and the corresponding lipid environment likely underwent mutual evolution and became functionally incompatible across the distant groups of microorganisms.

Tyrosine 75 is highly conserved in the EcoMscL subfamily of MscL channels, but its substitution by phenylalanine does not exert strong detrimental effects on

channel function either *in vivo* or in patch-clamp assays. It can not be excluded that this anchor increases only the fidelity of folding or assembly, but this conjecture has yet to be confirmed. Moving this tyrosine to position 93, analogous to Y87 of TbMscL (*34*) by the double Y75F/F93Y mutation produces a pronounced decrease in cell viability upon osmotic shock, which is correlated with a rightward shift of the activation curve by about 3 dynes/cm. This amount of shift should be considered large because the midpoint of 10 dynes/cm for WT MscL is already close to the lytic limit of the lipid bilayer (*38*) and further increases in activating tension must compromise the mechanical stability of the membrane as well as the survival. Introducing the second tyrosine Y93, in addition to the existing Y75, produced a similar right shift.

When two aromatic caps are present at positions 75 and 93, their residence in the carbonyl-populated layers in the opposite leaflets requires the M2 helices to be in a relatively upright position (Fig. 2). Tilting would retrieve one of the anchors from its favorable environment. Extending the distance between the periplasmic and cytoplasmic aromatic caps is expected to reduce the energetic cost of tilting. Indeed, moving the periplasmic cap to positions 98 or 102 partially restores the rescuing function of MscL. Peculiarly, the introduction of the second aromatic cap to the periplasmic side (I79W), although does not shift the activation midpoint as significantly, shortens the mean open time and severely compromises the osmotic function *in vivo* (Figs. 3 and 6).

Introduction of negatively charged glutamate in place of the single aromatic cap in the M2 helix (Y75E) prolongs the openings, only slightly increases the activation midpoint, and completely abolishes channel function *in vivo*, even with maximal protein expression (Fig. 3). Indeed, the right shift of activation in Y75E is less than in F93Y, but the detrimental effect on osmotic cell survival is more dramatic. An aromatic cap introduced on the periplasmic side of the M1 helix (I41W) reduces the activation midpoint, making the channel more sensitive to tension, and shortens the mean open time, but conspicuously leads to a complete loss of function *in vivo*. Previously, the amount of left shift in activation curves was shown to be correlated with toxic gain-of-function phenotypes. Although the severity of loss-of-function phenotypes generally correlates with a right shift of activation (Fig. 6), the behavior of Y75E, I79W and I41W shows that this correspondence does not always hold true. Therefore, both the tension midpoint and the mean open time are essential for function.

A change in activation tension may be related to the properties of aromatic residues. Partitioning of tryptophan analogs, 3-methylindole and indole between water and hydrocarbon or water and membrane indicated a stronger preference for membrane interface with a free energy difference of about –3 kcal/mole relative to cyclohexane, mostly enthalpic (*39*). Thus, the energy of transfer of five lipid-facing tryptophan side chains (one per subunit) from the interfacial layer into the hydrocarbon core can be roughly estimated as 15 kcal/mole (25 kT) at room temperature. To compare this energy difference to that of phenylalanine we can use another dataset from peptide partitioning measurements in water/octanol (mimicking

hydrocarbon) and water/membrane systems affected by the 'guest' residue. In these experiments W was found to be generally more hydrophobic than Y and F, with a slight preference for hydrocarbon as opposed to the interface ($\Delta\Delta G = -0.24$ kcal/mol). F exhibits a stronger preference for hydrocarbon ($\Delta\Delta G = -0.58$ kcal/mol). Y, the least hydrophobic of the three residues, prefers the interface as opposed to hydrocarbon ($\Delta\Delta G = +0.23$ kcal/mol). If we assume that gating is accompanied by a transfer of five such residues (one per subunit) from the interfacial carbonyl layer to the hydrocarbon core of the membrane, then Y and W substitutions should have effects of different magnitudes.

Based on the $\Delta\Delta G$'s, a replacement of F93 by Y should disfavor the open state by 4 kcal/mol (about 7 kT) for a pentamer. By the same inference, W at position 93 should exert an effect of only about 1.8 kcal/mol. Our experimental observations, however, suggest that apparent changes in gating energy are larger and very similar for Trp and Tyr substitutions. The shift of the tension midpoint, $\gamma_{1/2}$, reflects a proportional increase in the apparent energy of the opening transition (Fig. 5 and the legend). Given that the entire opening transition for WT MscL ($\gamma_{1/2} = 10.2$ dyn/cm) costs about 30 kcal/mol (50 kT), the substitutions that increase the $\gamma_{1/2}$ by 3 dyne/cm effectively destabilize the open state relative to the closed state by 9 kcal/mol. The Y and W substitutions at position 93 increase the gating energy by 8.7 and 8.1 kcal/mol, respectively; they also prolong the mean open time by about one order of magnitude, which is equivalent to the increase of the barrier for closing (i.e. energy of the transition state relative to the open state) by 1.7 kcal/mol.

Although we attempted to interpret the energetic effects of substitutions in terms of penalties associated with the transfer of a particular residue from the interfacial layer to the less polar hydrocarbon, other explanations should be considered. Flattening of the channel complex may cause a costly distortion of boundary lipids around the channel and the coupling of the channel conformational change to the bilayer deformations may depend on the presence of aromatic anchors. Extensive studies of model peptides WALP and KALP in membranes of different thickness by Killian and coworkers have demonstrated that tryptophans are powerful end-helix anchors which drive mutual adaptations of lipids and possibly peptides to prevent displacements of these residues from the interface. As evident from Fig. 5, tryptophan substitutions are more deleterious for osmotic viability than tyrosine substitutions. The increased distance between aromatic caps (L98W and L102W mutations) only partially restores rescuing ability and is highly consistent with the fact that strong tilting of long Trp-capped alpha helices (WALP 23) even in thin bilayers does not occur spontaneously. In the presence of Trp anchors, tilting appears to be more unfavorable than exposure to hydrophobic surfaces (hydrophobic mismatch) apparently because the former causes costly distortions of the more rigid interfacial layer of the membrane.

The large apparent changes in the free energy of opening caused by aromatic substitutions (8-9 kcal/mol) may not only reflect the actual change in the energy of transition, but also the way the external force is applied to the protein and transmitted from the lipid bilayer to the channel gate. Indeed, these mutations may change the character of protein-lipid interactions and the pressure/tension distribution at the

protein-lipid boundary. It has been suggested by several computational studies that the density of non-bonded interactions is highest in the polar layers of the membrane, and thus tension in the bilayer must be transmitted specifically through these peripheral regions. The altered distribution of forces at the protein-lipid boundary may drive the opening transition through a different (non-optimal) pathway, requiring a higher effective tension.

In conclusion, the *in vivo* osmotic rescuing ability of MscL is diminished by aromatic substitutions perturbing protein-lipid interactions at the ends of transmembrane helices. These mutations do not change the overall hydrophobicity of the protein-lipid interface, but likely perturb more subtle interactions arising from specific affinities of tyrosines and tryptophans to the interfacial regions of the lipid bilayer. Electrophysiological characterization of these mutants shows not only a general correspondence between the right shifts of activation curves and the reduction of osmotic rescuing efficiency, but also indicates drastic exceptions with no strict correlation between the two parameters. It appears that the structure of the lipid-facing surfaces in mechanosensitive channels is finely tuned to the specific lipid environment.

# Chapter 4: Dynamics of Pore Lining Helices in MscS

## *Introduction*

The phenomenology of MscS gating has been recently studied in our laboratory (*18*). By using patch clamp technique and a high speed pressure apparatus it has been shown that MscS expressed in *mcsS- E. coli* spheroplasts is steeply and reproducibly activated when stimulated by linear tension ramps. The activation of MscS is essentially voltage independent (*18*). When the channels are activated by the application of constant tension, the channel undergoes a time-dependent inactivation, which slows down upon increasing tension and as saturation is approached. Inactivation, on the other hand is strongly facilitated by depolarization.

The crystal structure of MscS was solved by Bass et al in 2002. The solved crystal structure of MscS (*16*) provides an opportunity to model the three functional states and envision the entire functional cycle. Molecular dynamics studies by Dr. Andriy Anishkin have indicated that the hydrophobic constriction of crystallized MscS (0.7 nm in diameter) is dehydrated and, contrary to the early notion that crystal structure represents the open state, the channel appears to be in a non-conductive, and possibly inactivated state.

The detached state of the lipid facing TM1 and TM2 helices from the pore forming TM3 helices suggests that the crystal state of the channel is irresponsive to membrane stretch, and may therefore be the inactivated state. From the crystal

structure Andriy has generated models of the closed state of the channel with the TM2 and TM3 helices tightly associated with TM3.

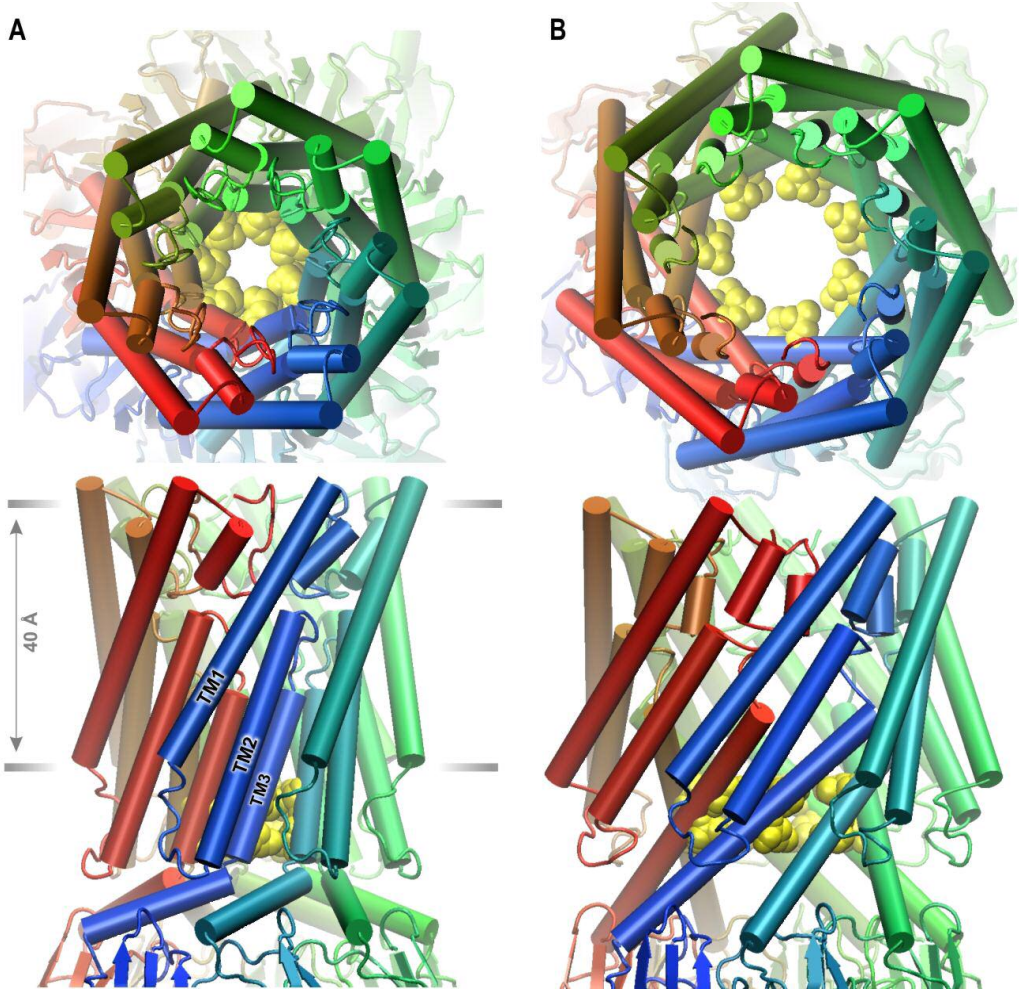


**Figure 7.** The hypothetical MscS gating transition. The models are derived from the crystal structure of MscS. In the closed state (A), more compact than the crystal structure TM3 helices remain in crystal-like positions. It was expanded in the open state in (B) using targeted minimization in NAMD.

The open state (B) was generated using several cycles of targeted energy minimizations and molecular dynamics simulations (Fig. 7). It satisfies the observed conductance of 1.2 nS, and has a ~12nm$^2$ larger in-plane area than that of the closed state (A). Unitary conductance estimations predict that the diameter of the narrow section of the pore must increase by 8-9 Å compared to that of the crystal structure which was shown to be closer to 7 Å. The gross in-plane protein expansion associated with the opening transition estimated from the slope of dose-response curves (ln (Po/Pc)$\gamma$) is 16-18nm$^2$.

The separation of the tightly packed TM3 helices is an important feature in this model. In order to satisfy the diameter of the conductive pore, the helices must move radially by 4-5 Å, which results in gaps between the complementary surfaces that are about 2-3 Å wide.

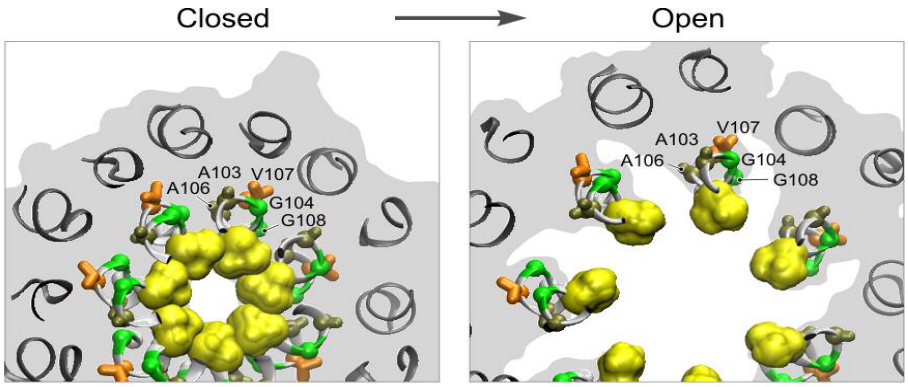


**Figure 8.** Cross-sections of the closed and open conformations through the gate region. Predicted positions of residues on TM3 segments are shown. Gate-keeping L105 sidechains are represented with yellow VdW surfaces. Predicted separation of TM3 helices increases the accessibilities of residues buried in the closed state.

The crystal structure of the open state shows a cylindrical pore region with L105 and 109 forming the hydrophobic constriction assigned as a gate. These bulky side-chains of L105 and L109 are shown in yellow. The TM3 helix, which lines the pore, is the most highly conserved region in MscS as is essentially hydrophobic (*15;16;40*). This region is composed of a repeating pattern of glycine and alanine residues in the following pattern: 98-AxxGAAGxAxGxAxyG-113 (x are hydrophobic residues and y is a hydrophilic residue) (*41*). Conserved alanines from one helix pack tightly against conserved glycines of the adjacent subunit (*4*).

The opening transition is illustrated by cross-sections of the closed and open states through the gate region in figure 8. In the closed state, TM3 helices are tightly packed with a knob-into-hole fashion and the pore wall has no visible gaps. The residues buried contacts, like G104 and A103, as well as residues facing outside, V107, are firmly isolated in the pore lumen. An expansion satisfying the open-state conductance clearly separates TM3 helices such that buried glycines and alanines become water exposed. Because glycine is very hydrophilic, it may be hydrated by water wedging in between the helices, where this water would strongly stabilize the expanded, open conformation. On the other hand, disruption of these interhelical contacts is also expected to increase helical dynamics such that buried sites and sites facing the outside, may have a higher probability of being exposed to the lumen and modified by an MTS reagent.

Stabilization of the open state by water hydrating glycines is an important prediction of the model. Edwards et al (*4*) recently published data showing that

G101, G104, and G108, substituted by alanines increases the pressure threshold of MscS activation, thus destabilizing the open state. Thus, alanine side-chains, grafted in perfectly complementary interhelical contacts, should push the helices apart towards the open conformation. Contrary to this expectation, they showed that a stronger destabilizing effect arose, apparently from an inability to hydrate the alanine portion of the helical backbone.

Because there are no cysteines in native MscS we can use Scanning Cysteine Accessibility Mutagenesis (SCAM) using Methanethiosulfonate (MTS) reagents to test and refine the open state conformation of MscS. MTS reagents bind specifically to cysteine residues that are exposed, in the closed state to those residues which are accessible or in the open state upon activation by hypotonic shock. MTS accessibility experiments thus can be used to probe the pore accessibilities of specific residues. The current open state model shows that all transmembrane helices are tightly packed around the central barrel in the resting state. Any expansion will separate the helices exposing alanines and glycines to water.

Our studies attempt to first test the predicted separation of TM3 helices in the course of the conformational transition and then to characterize the overall geometry of the open pore. It is important to determine whether the sites buried within TM3-TM3 contacts and those further from the pore constriction are inaccessible to water-soluble MTS reagents, and whether they become accessible upon channel activation. Using SCAM and cell viability assays, the majority of this region, residues 98-108 have been studied. Because many MTS modifications produce GOF channels, we

have performed osmotic viability experiments in the presence of MTS. Cell survival is expected to drop dramatically if a sensitive site is modified upon channel opening by the application of hypotonic shock. In parallel, accessibilities for each residue to MTS reagents have been tested in patch clamp experiments. Together this information can provide critical information not only possibly providing information to verify the spatial relationships of our model, but also to illustrate the dynamics of helices in MscS gating.

If a residue is exposed in the closed state, modification by a charged MTS reagent should occur with no applied shock. If this cysteine residue is close to the gate region, this modification may make the channel leaky, resulting in a toxic effect, consistent with low colony counts in plate assays. In patch clamp experiments, the effect of channel modification in the resting state should be observed prior to the application of activating pressure. If a residue is buried in the closed state, and only becomes exposed upon channel opening, the toxic effect of MTS should only be visible after shock. Changes in gating patterns associated with charged MTS modifications will become obvious only after first activating pressure pulses applied in the presence of the MTS reagent.

Our current model predicts that channel opening is associated with straightening of the characteristic kinks near G113 in each of the subunits, producing a conical structure tapering toward the periplasm. If the kink does not straighten, the pore may remain almost cylindrical. The double mutation A102L/L109A is predicted to move the hydrophobic constriction up one helical turn and should be instrumental

in testing the hypothesis of a conical pore expansion. If this is the case, moving the constriction up toward the periplasm would essentially make the pore region narrower and may require more tension to open. A similar conductance of this mutant would suggest a conical shape, while a decrease in conduction may suggest that in fact the pore lining helices are tilted and do form a tapered conical structure. Several mutants were created and tested by both osmotic shock and patch clamp characterization.

The A102L/L109A mutation is supposed to move the original constriction one helical pitch up, toward the periplasm. As shown in the model of this mutant with a tapered arrangement of TM3 helices, this modification makes the lumen of the pore smaller and predicts the decrease of conductance relative to WT MscS. The upper leucines (in this instance L102) are positioned slightly closer to each other and occlude the pore more. Therefore, introduction of valines characterized with slightly smaller side-chains in these positions is predicted to widen the pore. Thus the A102V/L109A mutant is predicted to have a slightly larger conductance than the A102L/L109A mutant.

## *Results and Discussion*

### *Determination of MTS Accessibility of TM3 Residues*

Ten mutations were generated using site-directed mutagenesis in the area lining the pore constriction of MscS. These TM3 residues include: A98C, V99C, L100C, G101C, A102C, A103C, G104C, A106C, V107C, and G108C. Two double

mutants were also generated in an attempt to move the gate up by one helical turn to test the hypothesis of the pore configuration which include: A102L/L109A and A102V/L109A. The mutations in the TM3 helix (residues 98-108) all attempt to determine the accessibilities of TM3 residues to MTS reagents. In order to test for

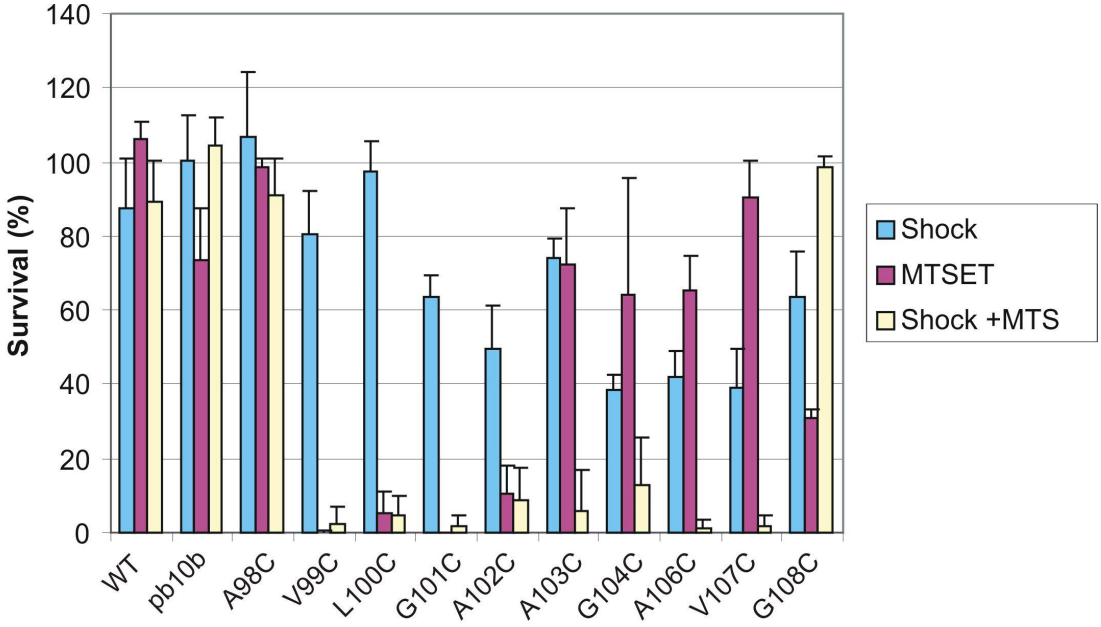


**Figure 9**. Osmotic survival of MJF 465 cells of TM3 residues including both WT and the empty vector control, pB10b under induced conditions with and without the presence of 0.6mM MTSET. Survival of MJF 465 cells expressing different MscS mutants upon a 400mOsM osmotic down shock. The effect of MTSET under non-shock conditions is shown in purple. Residues 98-102 seem accessible in the resting state, while cysteines in positions 103,104 and 106 are not accessible in the closed state but are modified quickly upon channel opening.

the expression levels of these mutants, western blots were done and it was determined that all cysteine mutants express at comparable levels, consistent with WT expression. Osmotic shock viability assays were done with and without the presence of MTSET, as well as a control of the effect of MTSET with no apparent shock, which should, in effect mimic WT.

As shown in figure 9 it can be seen that the addition of MTSET without any shock has a minimal effect, for most residues. A change in viability in the presence of MTS without shock identifies residues that are constitutively exposed to the lumen or other aqueous compartments in the resting state. Residues 99 to 102 may thus be exposed in the closed state because somehow MTS is able to bind and induce some sort of leaky channel, which causes a toxic (GOF) effect. A98C is presumably too far from the pore constriction to drastically effect channel parameters that would decrease cell viability. The characteristic changes in gating patterns in the presence of MTSET for A102C, A103C, G104C and A106C MscS (figure 10) show that the modified channels gate much faster and open at lower pressure, even exhibiting spontaneous activities. The most drastic effect was observed with the A106C mutation: MTSET modifying this residue on the first opening keeps the channel permanently open at a sub-conducting state without any applied pressure.

Patch clamp data for these residues directly correspond to data from cell viability assays. Residues 103-108 are not affected by MTS in the resting conformation, but become exposed and available for MTS to bind upon channel opening. These mutations slightly compromise the rescuing ability of MscS. The behavior of G108 is somewhat puzzling in that it is apparently modified by MTS and does not exhibit any drastic effect, despite its residence directly in the gate region. There is a strong correlation between the reduction of activating pressure on MTSET modification and toxicity. Therefore, it can be seen that all residues are accessible to

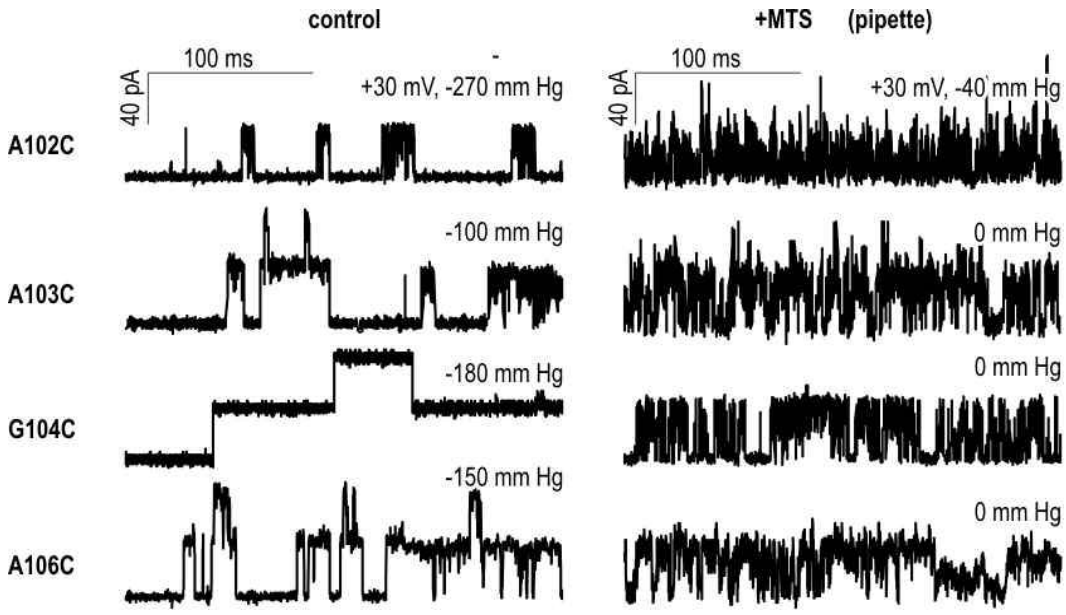


**Figure 10.** Traces of single-cysteine mutants in the gate region of TM3 recorded without and with positively charged MTSET (1 mM) in the pipette. The labeling drastically changes channel kinetics and pressure-sensitivity. A102C exposed in the closed state was labeled in state-independent manner, whereas other cysteines could be labeled only in the open state. Those events produced spontaneous activities without applied pressure.

MTSET in the activated (open) state, however, residues 103, 104, 106, and 107 seem to be accessible only in the event of an activating stimulus. It should be noted that the critical residues L105 and L109 were not modified because substitutions at this position are known to cause a strong GOF effect.

*Characterization of the Overall Geometry of the Open Pore*

Based on the analysis of the pore lining (*42*) residues L105 and L109 not only form the constriction, but also form both the narrowest and most hydrophobic part of the pore. As shown in figure 8, the model of the open state predicts that the

constriction is formed by the side chains of L105 and L109, as it is in the closed state, but the diameter of the constriction is 9Å wider (~17 Å) and therefore must be fully hydrated. The TM3 helices with straightened kinks near G113 are tilted, forming a funnel-like structure widening toward the cytoplasm. In a concurrent model of the open state (not shown), the TM3 helices still contain kinks and are almost parallel. One of the experimental strategies to discern between the two types of models (tapered vs. parallel) is to shift the constriction along the pore axis and see what effect it has on the conductance.

To test the hypothesis of a tapered pore geometry, we have introduced two mutations that move the hydrophobic constriction (gate) from the cytoplasmic end of the transmembrane pore toward the periplasm by one helical turn. If the pore were strictly cylindrical we would observe no change in conductance. However, we predict that the pore expansion is conical and expect to see a reduction in conductance upon channel opening in the mutant channels (Figure 11).

Figure 11 illustrates the hypothetical arrangement of the helices and the gate keeping aliphatic residues in WT MscS and the two mutants. A102L/L109A, in which the gate is moved one helical turn up the pore (L102 and L105 now forms the constriction instead of L105 and L109). The A102L/L109A and A102V/L109A mutants of MscS were generated using the Quick-change mutagenesis kit and verified by automated sequencing. The mutants expressed in pB104 (*mscL-, mscS-*) cells showed no GOF growth phenotype. Their osmotic survival is currently being tested.

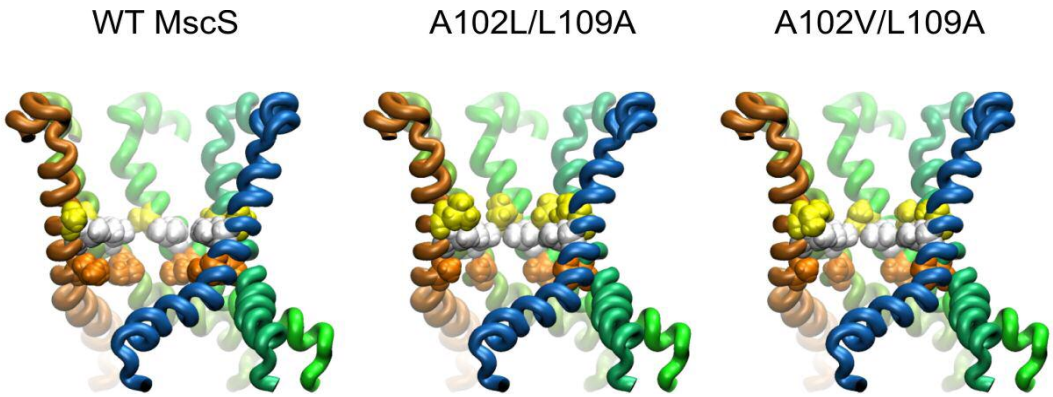


**Figure 11.** Arrangement of helices and gate keeping aliphatic residues in MscS and A102L/L109A and A102V/L109A. The first mutation is predicted to reduce the cross-sectional area of the pore from 16 to ~12nm$^2$.

Patch clamp experiments performed on giant spheroplasts revealed mechanosensitive channel activities in both preparations. The level of expression of each of the mutants was lower (5-20 channels per patch) than in spheroplasts expressing WT MscS (30-60 channels per patch). Single-channel traces recorded at different voltages provided clearly resolvable unitary conductances (Fig. 12, left), from which current-to-voltage relationships (I-V curves) could be plotted, with the slopes defining unitary conductances in each case. The I-V curves for WT, A102V/L109A, and A102L/L109A MscS are presented in Fig. 12, right, show that the unitary channel conductances are indeed smaller in these mutants. Moving the gate formed by two rings of leucines one helical pitch up the pore reduces the unitary conductance from 1.34 to 0.66 nS, i.e. by 51%. Replacement of the upper leucine (L102) by valine incurs a 40% reduction of conductance (from 1.34 to 0.81 nS) relative to WT, clearly illustrating that the side-chains of these aliphatic residues in

the open conformation remain in the pore (and do not swing out) as their volume influences the conductance.

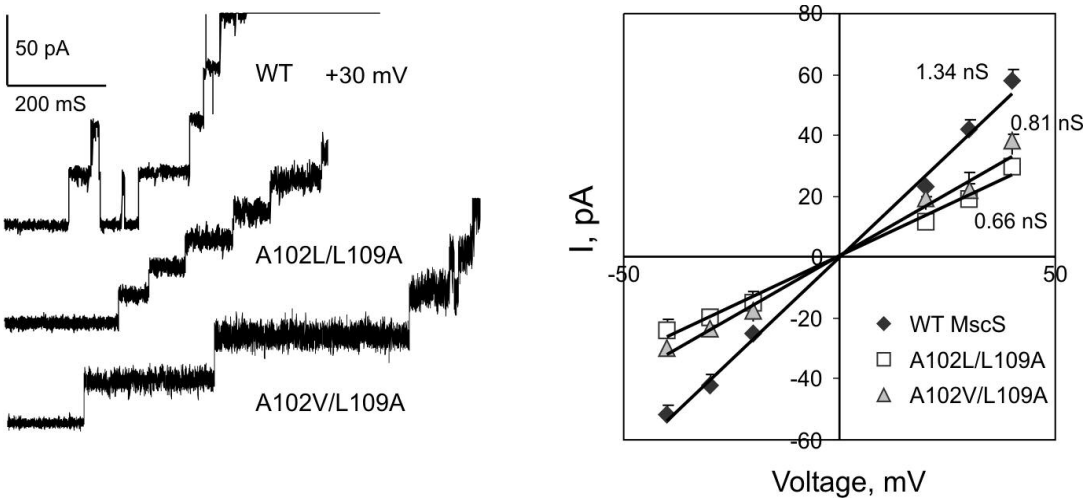


**Figure 12**. (left) Traces of the two mutants as compared to WT MscS and (right) current-to-voltage relationships for WT MscS and two mutants with the hydrophobic constriction (gate) moved toward the periplasmic side. The A102L/L109A mutation moves the two gate-keeping leucines up by one helical turn and reduces the conductance by 51%. When L102 is replaced by valine, only a 40% conductance is seen, indicating that these residues protrude into the pore and that the volume directly defines the cross-section of the conductive lumen of the pore.

The data is more consistent with the tapering pore model of the open state. It might be premature to try to deduce the exact angle of helical taper from these measurements, but the model predicts that the tilt angle might be close to $40^{o}$ relative to the pore axis. More experiments would be required to elucidate the functional role of the gate position in the mechanism of MscS, and one of them is to move the gate two helical turns up the pore. Models and short MD simulations of altered pores as

well as conductance calculations based on the averaged position of helices and side-chains will assist the data analysis.

*Conclusions*

Bacterial growth parameters and plate phenotypes are used to probe many aspects of cell physiology, including membrane transport and osmotic adaptation. We have used bacterial cell survival as a tool to determine and analyze the effects of channel function *in vivo* in both MscL and MscS. Used in combination with electrophysiological techniques and structural approaches, plate phenotyping has become a powerful tool for probing molecular mechanisms and has allowed us to address biophysical questions regarding the function of these molecular components, bacterial turgor regulation systems. I have focused primarily on two aspects of mechanosensitive channel function in bacteria by introducing and analyzing mutations in functionally important regions of both channels.

Sharing no homology or structural similarity (*8;15;41*), both channels work to rescue cells from lysis upon the onset of osmotic shock manifested as increased turgor pressure. This system provides a graded response with MscS activating first, and then MscL, activating at extreme pressures approaching the lytic limit of the membrane. The large conductance of MscL implies a large-scale conformational change. It is now apparent that the gating of MscL is a result of an iris-like opening accompanied with membrane expansion due to the outward movement of the helices

(*11*). The overall in-plane area change associated with the closed to open transition is about 23nm$^2$ and this transition increases the tilt of the helices from 32 to 71 degrees relative to normal (*12*).

The lipid facing helices and more specifically, groups exposed to membrane polar/apolar interfaces of MscL were targeted in the first part of my study. The motivation arose from sequence analysis showing a conspicuous absence of aromatic anchors on both sides of lipid facing helices. Tyrosines and tryptophans are common near the membrane surface of most membrane proteins. It has been suggested that the polar character of the tryptophan amide group and the tyrosine hydroxyl, along with their hydrophobic ring structures, suit them for localization at the polar/apolar interface amid the glycerols and carbonyls of phospholipids. However, because of the transition required for MscL gating, such aromatic residues appear to be a hindrance to channel opening due to the helical reorientation that is required. The addition of aromatic residues, in effect, strains the channel from undergoing this type of rearrangement, which is manifested upon osmotic survival assays and verified through patch clamp experiments. The channel, if it opens at all becomes more difficult to open or will open at a much greater tension.

Therefore, it can be concluded that MscL, in contrast to most membrane proteins, does not have aromatic residues at both polar/apolar interfaces because of the conformational change that is required upon channel opening. This large scale conformational change not only implies and expansion, but also a flattening or thinning of the MscL protein. Unless the membrane deforms dramatically, the

capping groups likely change their environment and therefore the chemical nature of the side chains becomes important. The results demonstrate that the introduction of specific interactions with lipids may restrain the gating transition and this is highly consistent with the iris-like model of channel opening. It emphasizes the role of protein-lipid interactions in channel gating energetics, stimulating further studies in this direction.

The gating mechanism of MscS is far less understood. Although several models exist, more experimentation is required in order to verify the exact conformation of the channel in the membrane. It is not apparent what conformational state the current model represents. As a result of our experiments we have determined that not only is the structure published by the Rees group most likely an inactivated state and not the true open state as proposed, but also that the dynamics of channel opening occurs in a conical, rather than cylindrical fashion. The crystal structure is static and provides no direct information about the dynamics of channel opening. Our experiments have served to verify our current model and have allowed us to determine which residues are accessible in the closed state, and those which are only accessible upon channel opening.

My experiments regarding cysteine accessibility in the TM3 helix of MscS demonstrate that the entire helical stretch between residues 98 to 108 become accessible through the lumen upon channel activation. This indicated that the pore-lining helices no longer create a tightly packed wall and must separate. Thus, expansion of the channel pore is required upon channel opening. In addition, TM3-

TM3 cross-links that stabilize the crystal-like conformation lock the channel in a non-conductive state, and upon reduction the channel may become activated by the application of sufficient tension. Using these techniques we have been able to understand the overall packing and mobility of these residues in both the closed and open states.

Additional information was obtained by moving the hydrophobic constriction one helical pitch toward the periplasm. The channels were functional in electrophysiological experiments, but demonstrated a lower conductance, consistent with the tapering model of the open pore. The replacement of leucine in position 102 by valine slightly increased the conductance, indicating that the aliphatic side chains of the gate-keeping residues remain in the lumen in the open state and do not swing out. Data from osmotic survival assays and patch clamp experiments is highly consistent with the radial separation of the pore-lining helices during the MscS gating transition, which is the key event in our model.

References


1. Hamill, O. P. and Martinac, B. (2001) Molecular basis of mechanotransduction in living cells, *Physiol Rev. 81*, 685-740.

2. Levina, N., Totemeyer, S., Stokes, N. R., Louis, P., Jones, M. A., and Booth, I. R. (1999) Protection of Escherichia coli cells against extreme turgor by activation of MscS and MscL mechanosensitive channels: identification of genes required for MscS activity, *EMBO J. 18*, 1730-1737.

3. Sukharev, S. I., Blount, P., Martinac, B., Blattner, F. R., and Kung, C. (1994) A large-conductance mechanosensitive channel in E. coli encoded by mscL alone, *Nature 368*, 265-268.

4. Edwards, M. D., Li, Y., Kim, S., Miller, S., Bartlett, W., Black, S., Dennison, S., Iscla, I., Blount, P., Bowie, J. U., and Booth, I. R. (2005) Pivotal role of the glycine-rich TM3 helix in gating the MscS mechanosensitive channel, *Nat. Struct. Mol. Biol. 12*, 113-119.

5. Wood, J. M. (1999) Osmosensing by bacteria: signals and membrane-based sensors, *Microbiol. Mol. Biol. Rev. 63*, 230-262.

6. Ashcroft, F. M. (2005) *Ion Channels and Disease* Academic Press, New York.

7. Maurer, J. A. and Dougherty, D. A. (2001) A high-throughput screen for MscL channel activity and mutational phenotyping, *Biochim. Biophys. Acta 1514*, 165-169.

8. Booth, I. R. and Louis, P. (1999) Managing hypoosmotic stress: aquaporins and mechanosensitive channels in Escherichia coli, *Curr. Opin. Microbiol. 2*, 166-169.

9. Sukharev, S. I., Sigurdson, W. J., Kung, C., and Sachs, F. (1999) Energetic and spatial parameters for gating of the bacterial large conductance mechanosensitive channel, MscL, *J. Gen. Physiol 113*, 525-540.

10. Moe, P. C., Blount, P., and Kung, C. (1998) Functional and structural conservation in the mechanosensitive channel MscL implicates elements crucial for mechanosensation, *Mol. Microbiol. 28*, 583-592.

11. Sukharev, S., Betanzos, M., Chiang, C. S., and Guy, H. R. (2001) The gating mechanism of the large mechanosensitive channel MscL, *Nature 409*, 720-724.

12. Sukharev, S., Durell, S. R., and Guy, H. R. (2001) Structural models of the mscl gating mechanism, *Biophys. J. 81*, 917-936.

13. Perozo, E., Cortes, D. M., Sompornpisut, P., Kloda, A., and Martinac, B. (2002) Open channel structure of MscL and the gating mechanism of mechanosensitive channels, *Nature 418*, 942-948.

14. Perozo, E., Kloda, A., Cortes, D. M., and Martinac, B. (2002) Physical principles underlying the transduction of bilayer deformation forces during mechanosensitive channel gating, *Nat. Struct. Biol. 9*, 696-703.

15. Pivetti, C. D., Yen, M. R., Miller, S., Busch, W., Tseng, Y. H., Booth, I. R., and Saier, M. H., Jr. (2003) Two families of mechanosensitive channel proteins, *Microbiol. Mol. Biol. Rev. 67*, 66-85, table.

16. Bass, R. B., Strop, P., Barclay, M., and Rees, D. C. (2002) Crystal structure of Escherichia coli MscS, a voltage-modulated and mechanosensitive channel, *Science 298*, 1582-1587.

17. Anishkin, A. and Sukharev, S. (2004) Water dynamics and dewetting transitions in the small mechanosensitive channel MscS, *Biophys. J. 86*, 2883-2895.

18. Akitake, B., Anishkin, A., and Sukharev, S. (2005) The "dashpot" mechanism of stretch-dependent gating in MscS, *J. Gen. Physiol 125*, 143-154.

19. Koprowski, P. and Kubalski, A. (2003) C termini of the Escherichia coli mechanosensitive ion channel (MscS) move apart upon the channel opening, *J. Biol. Chem. 278*, 11237-11245.

20. Grajkowski, W., Kubalski, A., and Koprowski, P. (2005) Surface changes of the mechanosensitive channel MscS upon its activation, inactivation, and closing, *Biophys. J. 88*, 3050-3059.

21. Ou, X., Blount, P., Hoffman, R. J., and Kung, C. (1998) One face of a transmembrane helix is crucial in mechanosensitive channel gating, *Proc. Natl. Acad. Sci. U. S. A 95*, 11471-11475.

22. Blount, P., Sukharev, S. I., Schroeder, M. J., Nagle, S. K., and Kung, C. (1996) Single residue substitutions that change the gating properties of a mechanosensitive channel in Escherichia coli, *Proc. Natl. Acad. Sci. U. S. A 93*, 11652-11657.

23. Blount, P., Schroeder, M. J., and Kung, C. (1997) Mutations in a bacterial mechanosensitive channel change the cellular response to osmotic stress, *J. Biol. Chem. 272*, 32150-32157.

24. Yoshimura, K., Batiza, A., Schroeder, M., Blount, P., and Kung, C. (1999) Hydrophilicity of a single residue within MscL correlates with increased channel mechanosensitivity, *Biophys. J. 77*, 1960-1972.

25. Anishkin, A., Chiang, C. S., and Sukharev, S. (2005) Gain-of-function mutations reveal expanded intermediate states and a sequential action of two gates in MscL, *J. Gen. Physiol 125*, 155-170.

26. Bartlett, J. L., Levin, G., and Blount, P. (2004) An in vivo assay identifies changes in residue accessibility on mechanosensitive channel gating, *Proc Natl Acad Sci U S A 101*, 10161-10165.

27. Karlin, A. and Akabas, M. H. (1998) Substituted-cysteine accessibility method, *Methods Enzymol. 293*, 123-145.

28. Batiza, A. F., Kuo, M. M., Yoshimura, K., and Kung, C. (2002) Gating the bacterial mechanosensitive channel MscL invivo, *Proc Natl Acad Sci U S A 99*, 5643-5648.

29. Li, Y., Wray, R., and Blount, P. (2004) Intragenic suppression of gain-of-function mutations in the Escherichia coli mechanosensitive channel, MscL, *Mol. Microbiol. 53*, 485-495.

30. Yoshimura, K., Nomura, T., and Sokabe, M. (2004) Loss-of-function mutations at the rim of the funnel of mechanosensitive channel MscL, *Biophys. J. 86*, 2113-2120.

31. Yoshimura, K., Batiza, A., and Kung, C. (2001) Chemically charging the pore constriction opens the mechanosensitive channel mscl, *Biophys. J. 80*, 2198-2206.

32. Martinac, B., Buechner, M., Delcour, A. H., Adler, J., and Kung, C. (1987) Pressure-sensitive ion channel in Escherichia coli, *Proc. Natl. Acad. Sci. U. S. A 84*, 2297-2301.

33. Chang, G, Spencer, R.H. , Lee, A.T., Barclay, M.T., and Rees D.C., (1998)*Structure of the MscL homolog from Mycobacterium tuberculosis: a gated mechanosensitive ion channel,* 282 ed., pp 2220-2226.

34. Rees, D. C., Chang, G., and Spencer, R. H. (2000) Crystallographic analyses of ion channels: lessons and challenges, *J. Biol. Chem. 275*, 713-716.

35. Maurer, J. A. and Dougherty, D. A. (2003) Generation and evaluation of a large mutational library from the Escherichia coli mechanosensitive channel of large conductance, MscL: implications for channel gating and evolutionary design, *J. Biol. Chem. 278*, 21076-21082.

36. Moe, P. and Blount, P. (2002) A novel approach for probing protein-lipid interactions of MscL, a membrane-tension-gated channel., in *Biophysical chemistry; membranes and proteins* (Templer, R. and Leatherbarrow, R., Eds.) pp 199-207, Royal Society of Chemistry.

37. Levin, G. and Blount, P. (2004) Cysteine Scanning of MscL Transmembrane Domains Reveals Residues Critical for Mechanosensitive Channel Gating, *Biophys. J. 86*, 2862-2870.

38. Moe, P. C., Levin, G., and Blount, P. (2000) Correlating a protein structure with function of a bacterial mechanosensitive channel, *J. Biol. Chem. 275*, 31121-31127.

39. White, S. H. and Wimley, W. C. (1999) Membrane protein folding and stability: physical principles, *Annu. Rev. Biophys. Biomol. Struct. 28*, 319-365.

40. Miller, S., Edwards, M. D., Ozdemir, C., and Booth, I. R. (2003) The closed structure of the MscS mechanosensitive channel. Cross-linking of single cysteine mutants, *J. Biol. Chem. 278*, 32246-32250.

41. Perozo, E. and Rees, D. C. (2003) Structure and mechanism in prokaryotic mechanosensitive channels, *Curr. Opin. Struct. Biol. 13*, 432-442.

42. Sukharev, S. and Anishkin, A. (2004) Mechanosensitive channels: what can we learn from 'simple' model systems?, *Trends Neurosci. 27*, 345-351.

*Chemical structure of MTSET taken from http://chemfinder.com